Radio Loudness of Early-type Galaxies at Low and Very Low Radio Luminosity Range

Anna Wójtowicz et al.

Astronomical Observatory of the Jagiellonian University

Preliminary results- work in progress, all comments and suggestions are highly welcome!

The X-Ray Halo Scaling Relations of Supermassive Black Holes

M. Gaspari[1,20,21], D. Eckert[2], S. Ettori[3,4], P. Tozzi[5], L. Bassini[6,7], E. Rasia[6,8], F. Brighenti[9], M. Sun[10]
S. Borgani[6,7,8,11], S. D. Johnson[1,12,22], G. R. Tremblay[13], J. M. Stone[1], P. Temi[14], H.-Y. K. Yang[15,16]
F. Tombesi[15,17,18,19], and M. Cappi[3]

a unique collection of high-quality optical and X-ray data for nearby 85 galaxies, for which

- the masses of central SMBHs have been measured with high precision via direct dynamical methods, i.e. by resolving the stellar or gas kinematics within the SMBH influence regions (1–100 pc) ;
- the main galaxy parameters including the stellar velocity dispersion, the bulge mass, and the total galaxy K-band luminosity, were known;
- the intragroup/intracluster halo parameters, including the total halo luminosity and temperature, could be estimated with high precision from high-resolution X-ray imaging data (Chandra and XMM-Newon).

The overwhelming majority of the galaxies in the sample — 76 systems out of 85 total — are **early-type objects**, i.e. galaxies of the morphological Hubble types encompassing ellipticals (E0 - E6) and lenticulars (S0 - SAB0), at **distances between 3.6 and 152.4 Mpc**.

The large-scale environment of those ranges from **the centers of rich clusters, to poor galaxy groups, fields, and even isolated systems.**

The sample includes a **mixture of non-active and active galaxies**, unbiased with respect to the level of the jet activity.

The X-Ray Halo Scaling Relations of Supermassive Black Holes

M. Gaspari[1,20,21], D. Eckert[2], S. Ettori[3,4], P. Tozzi[5], L. Bassini[6,7], E. Rasia[6,8], F. Brighenti[9], M. Sun[10], S. Borgani[6,7,8,11], S. D. Johnson[1,12,22], G. R. Tremblay[13], J. M. Stone[1], P. Temi[14], H.-Y. K. Yang[15,16], F. Tombesi[15,17,18,19], and M. Cappi[3]

GASPARI ET AL. (2019): a unique collection of high-quality optical and X-ray data for nearby 85 galaxies, for which

(i) the masses of central SMBHs have been measured with high precision via direct dynamical methods, i.e. by resolving the stellar or gas kinematics within the SMBH influence regions;
(ii) the main galaxy parameters including the stellar velocity dispersion, the bulge mass, and the total galaxy K-band luminosity, were known;
(iii) the intragroup/intracluster halo parameters, including the total halo luminosity and temperature, could be estimated with high precision from high-resolution X-ray imaging data (Chandra and XMM-Newon).

The overwhelming majority of the galaxies in the sample — 76 systems out of 85 total — are **early-type objects**, i.e. galaxies of the morphological Hubble types encompassing ellipticals (E0 - E6) and lenticulars (S0 - SAB0), at **distances between 3.6 and 152.4 Mpc**.

The large-scale environment of those ranges from **the centers of rich clusters, to poor galaxy groups, fields, and even isolated systems.**

The sample includes a **mixture of non-active and active galaxies**, unbiased with respect to the level of the jet activity.

The main objective of Gaspari et al. (2019) was to research the link between SMBHs and their large-scale (galactic and intragroup/intracluster) environment.

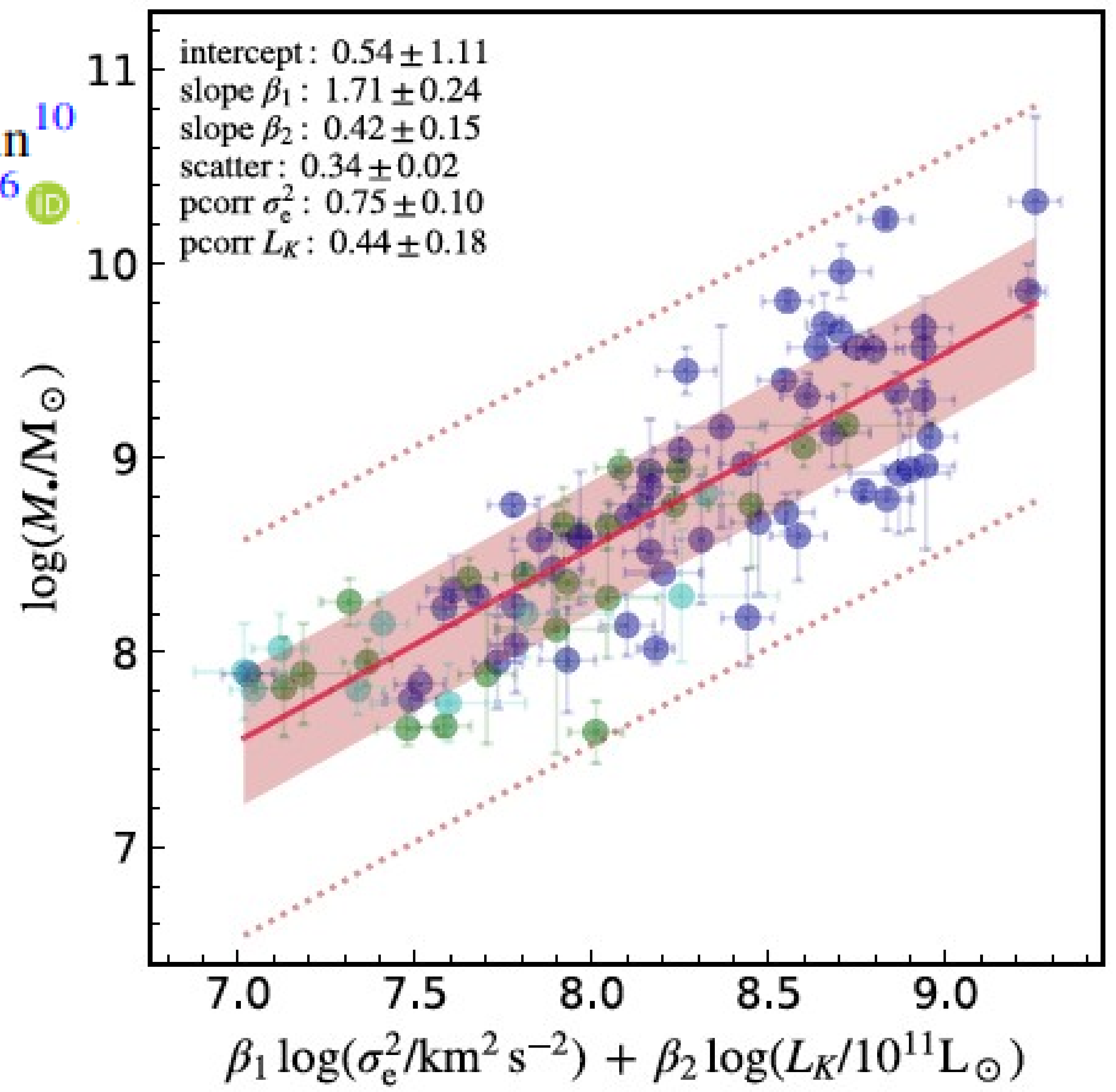

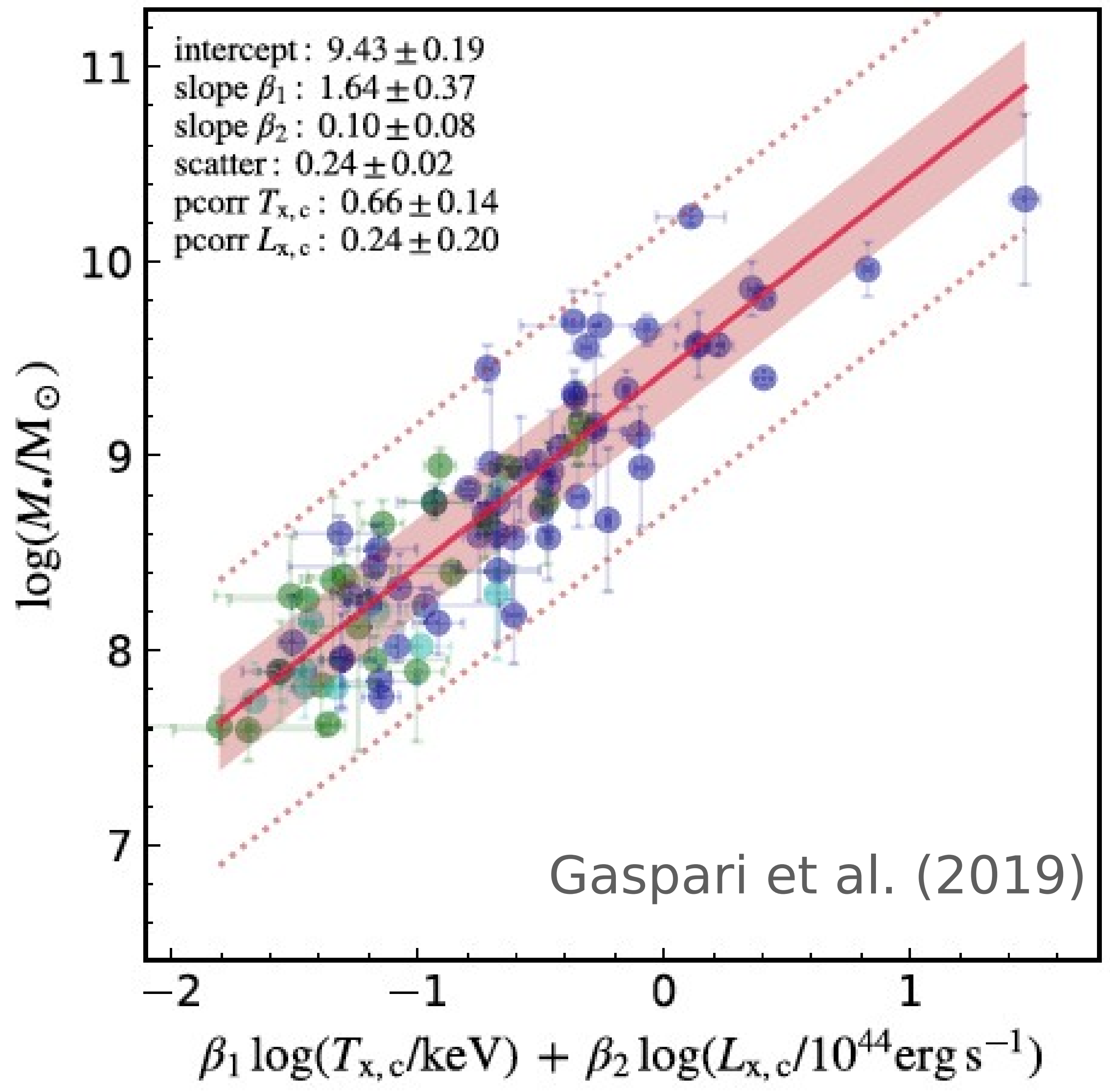

GASPARI ET AL. (2019):
a unique collection of high-quality optical and X-ray data for nearby 85 galaxies, for which

- the masses of central SMBHs have been measured with high precision via direct dynamical methods, i.e. by resolving the stellar or gas kinematics within the SMBH influence regions;
- the main galaxy parameters including the stellar velocity dispersion, the bulge mass, and the total galaxy K-band luminosity, were known;
- the intragroup/intracluster halo parameters, including the total halo luminosity and temperature, could be estimated with high precision from high-resolution X-ray imaging data (Chandra and XMM-Newon).

The overwhelming majority of the galaxies in the sample — 76 systems out of 85 total — are **early-type objects**, i.e. galaxies of the morphological Hubble types encompassing ellipticals (E0 - E6) and lenticulars (S0 - SAB0), at **distances between 3.6 and 152.4 Mpc, (z<0.04)**.

The large-scale environment of those ranges from **the centers of rich clusters, to poor galaxy groups, fields, and even isolated systems.**

The sample includes a **mixture of non-active and active galaxies**, unbiased with respect to the level of the jet activity.

The main objective of Gaspari et al. (2019) was to research the link between SMBHs and their large-scale (galactic and intragroup/intracluster) environment.

The** goal of our work **is to extend the analysis** to the radio **range, i.e. to investigate the radio emission of the uniquely gathered sample of galaxies.

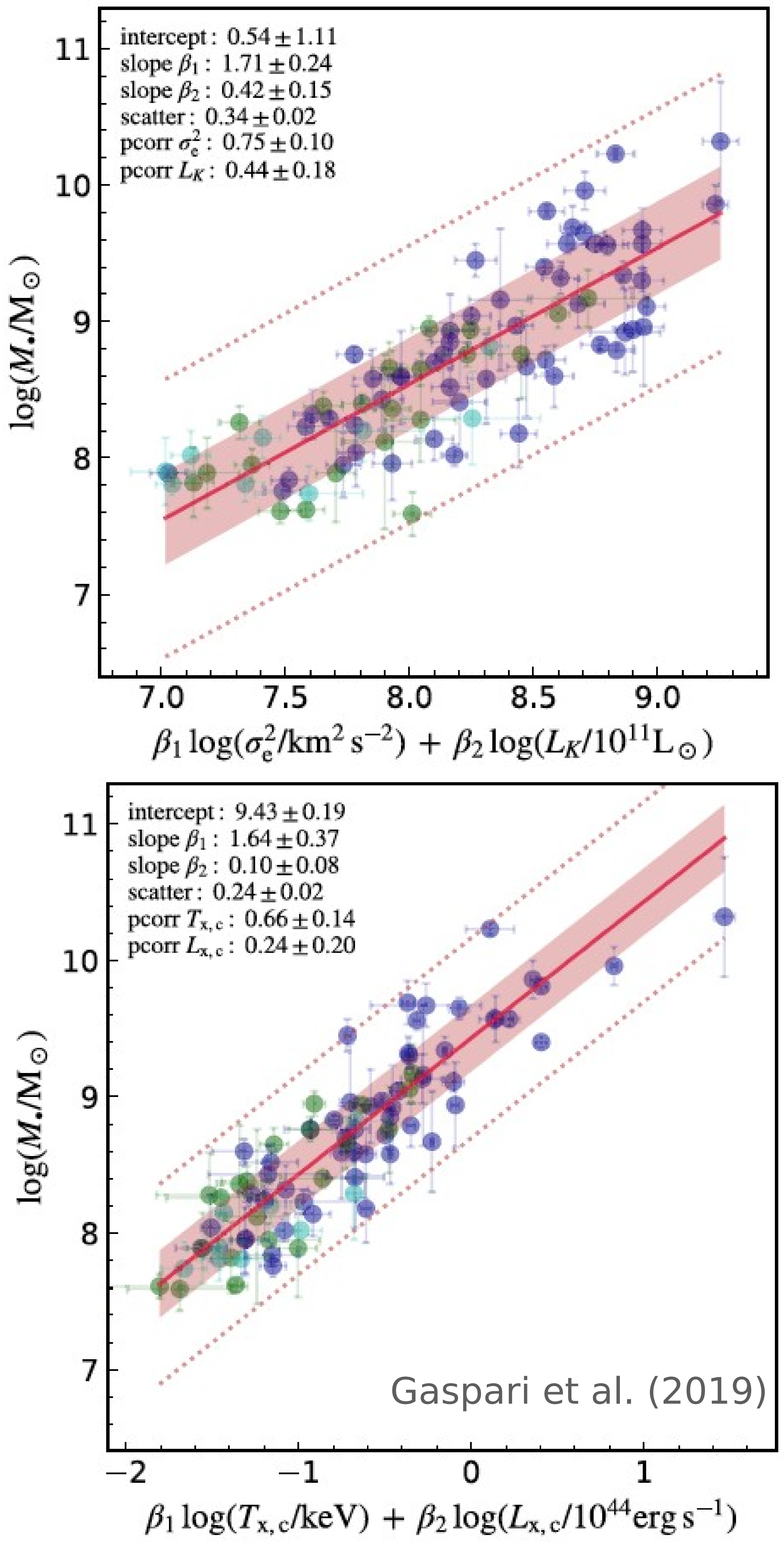

We collected the following data:

1) ***Integrated radio fluxes*** from the Very Large Array (VLA) observations ***at 1.4 GHz with 45'' resolution***, as cataloged in Condon et al. (1998, 2002) and Brown et al. (2011), plus several complementary observations for the southernmost sources from Allison et al. (2014).

2) ***High-resolution X-ray*** measurements of galactic nuclei (the innermost 2.5'') following from the Chandra archival data, as presented in She et al. (2017).

3) ***The total far-infrared fluxes at 100um and 60um*** from the Infrared Astronomical Satellite (***IRAS***) archival data (with 1.5' resolution at 60 um; 3' at 100 um)

Results:

First impression:

No particular patterns emerge except of some weaker correlations, e.g., L_r vs L_K …

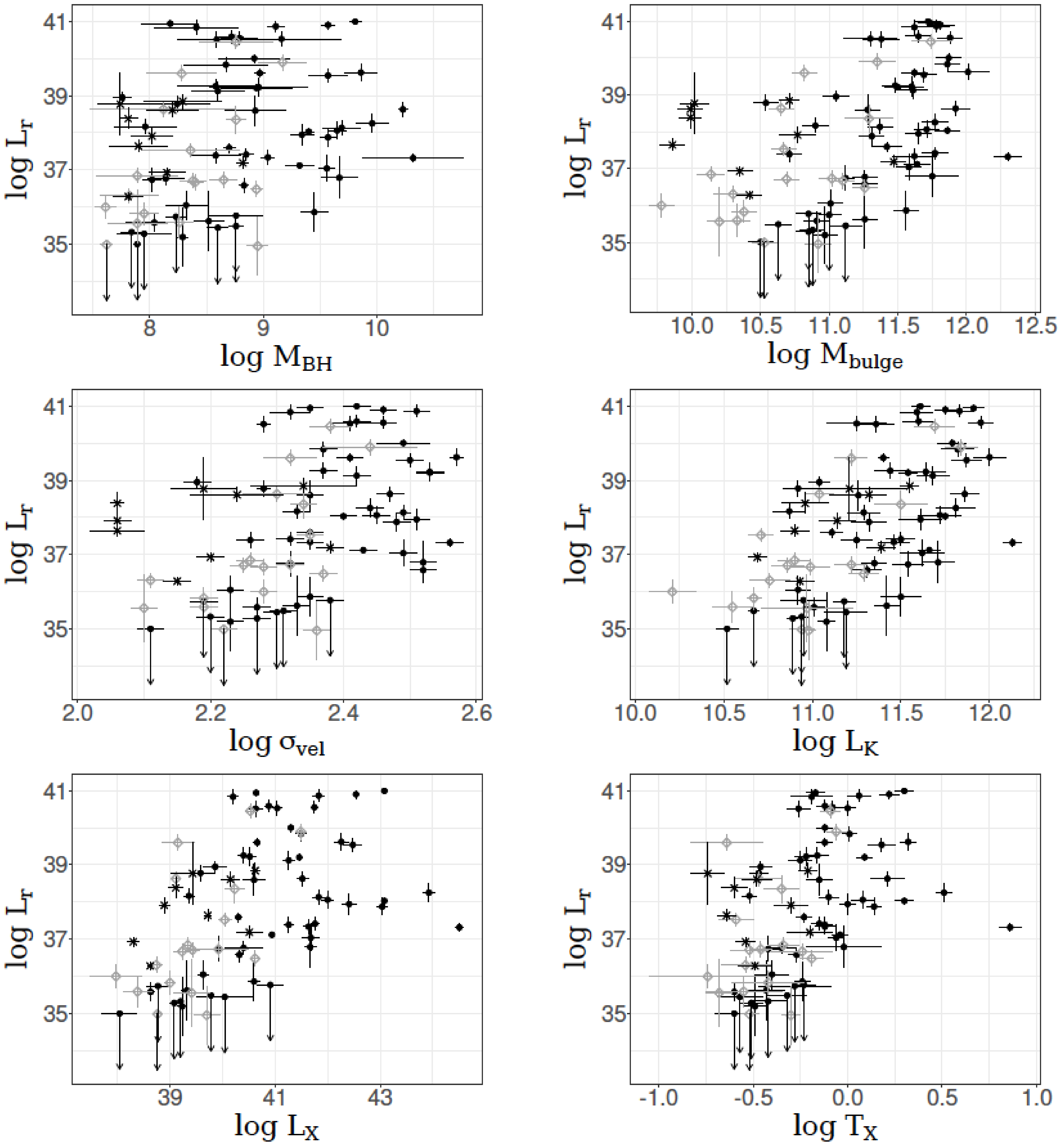

The black dots mark elliptical galaxies, grey empty squares lenticular galaxies, black stars spiral galaxies

RESULTS:

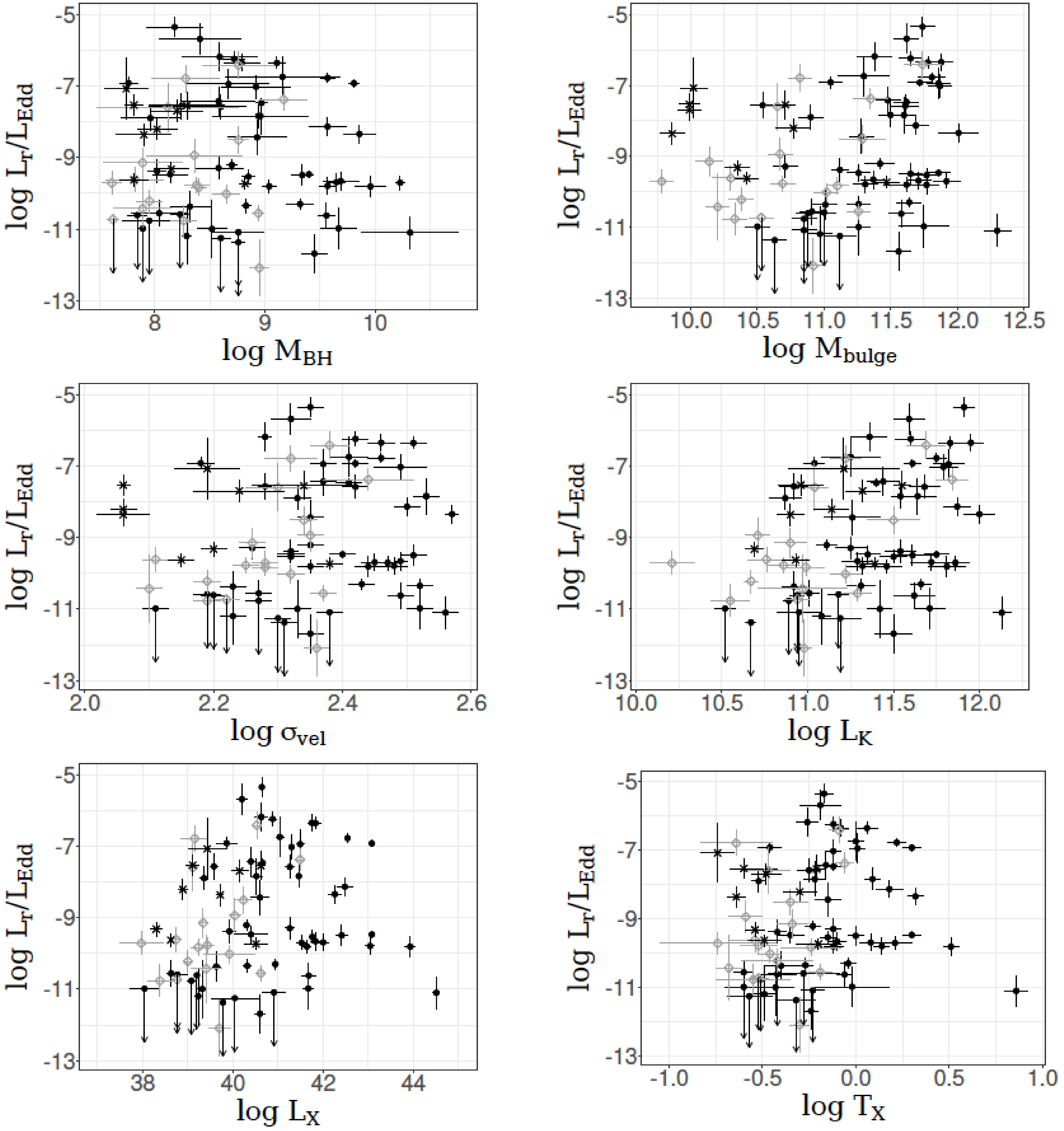

The black dots mark elliptical galaxies, grey empty squares lenticular galaxies, black stars spiral galaxies

First impression:

Much less significant correlation when L_r is expressed in Eddington units

RESULTS:

However…

A closer inspection reveals a clear separation between “radio-dim” and “radio-bright” early-type galaxies

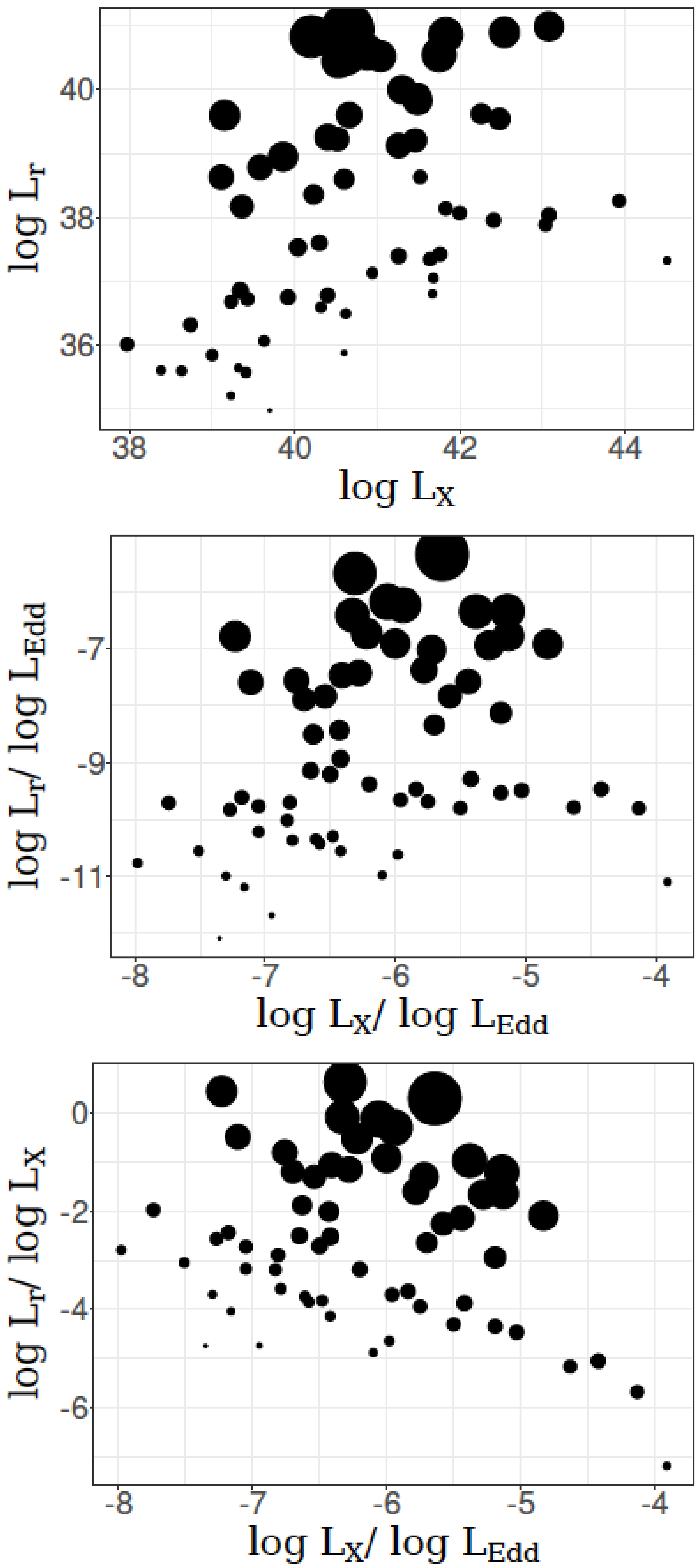

Graph for early-type sources only; the size of the points reflects L_r/L_Edd

Results:

However…

A closer inspection reveals a clear separation between “radio-dim” and “radio-bright” early-type galaxies

Is there a bi-modal distribution ?!

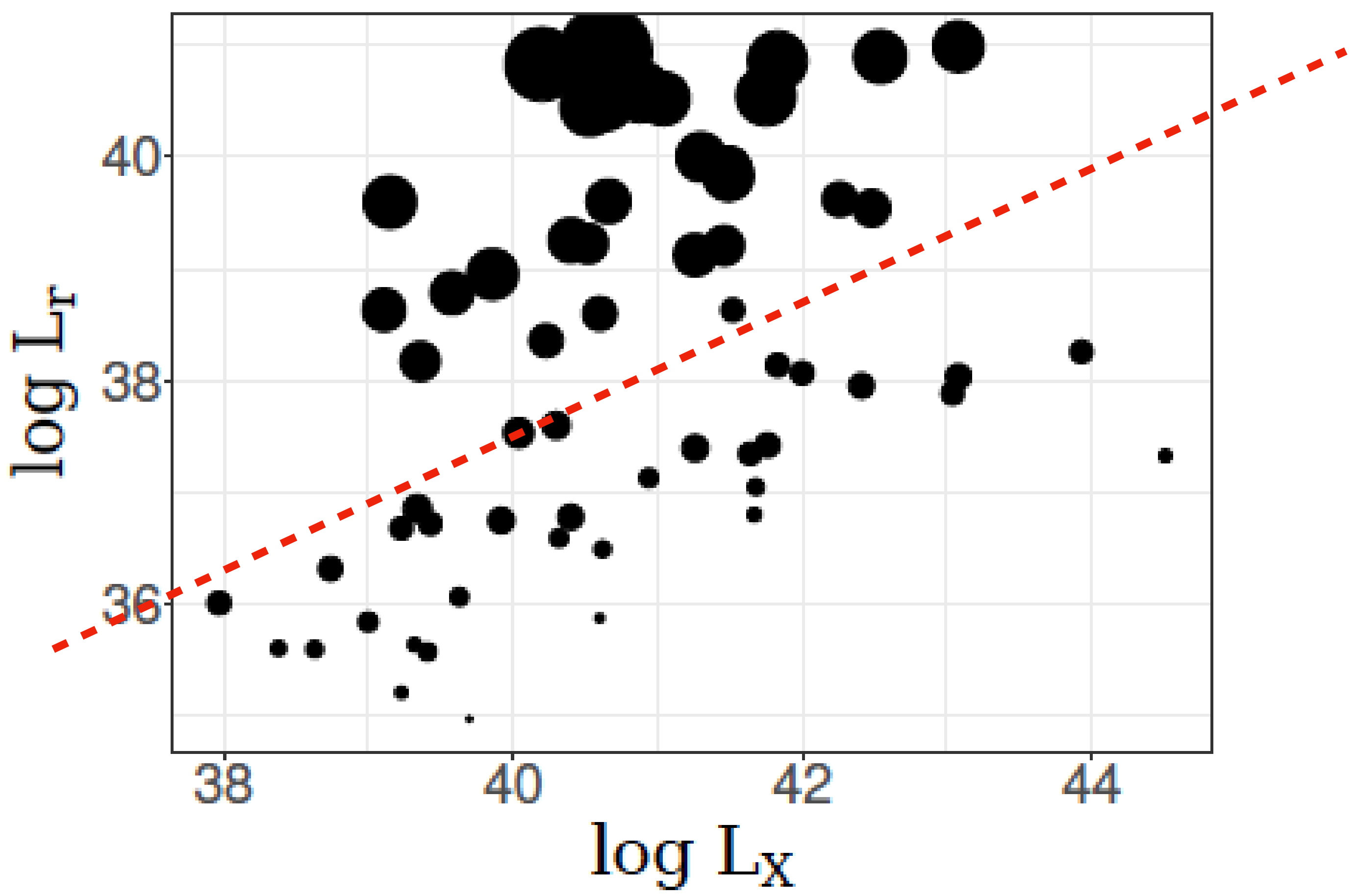

Graph for early-type sources only; the size of the points reflects L_r/L_Edd

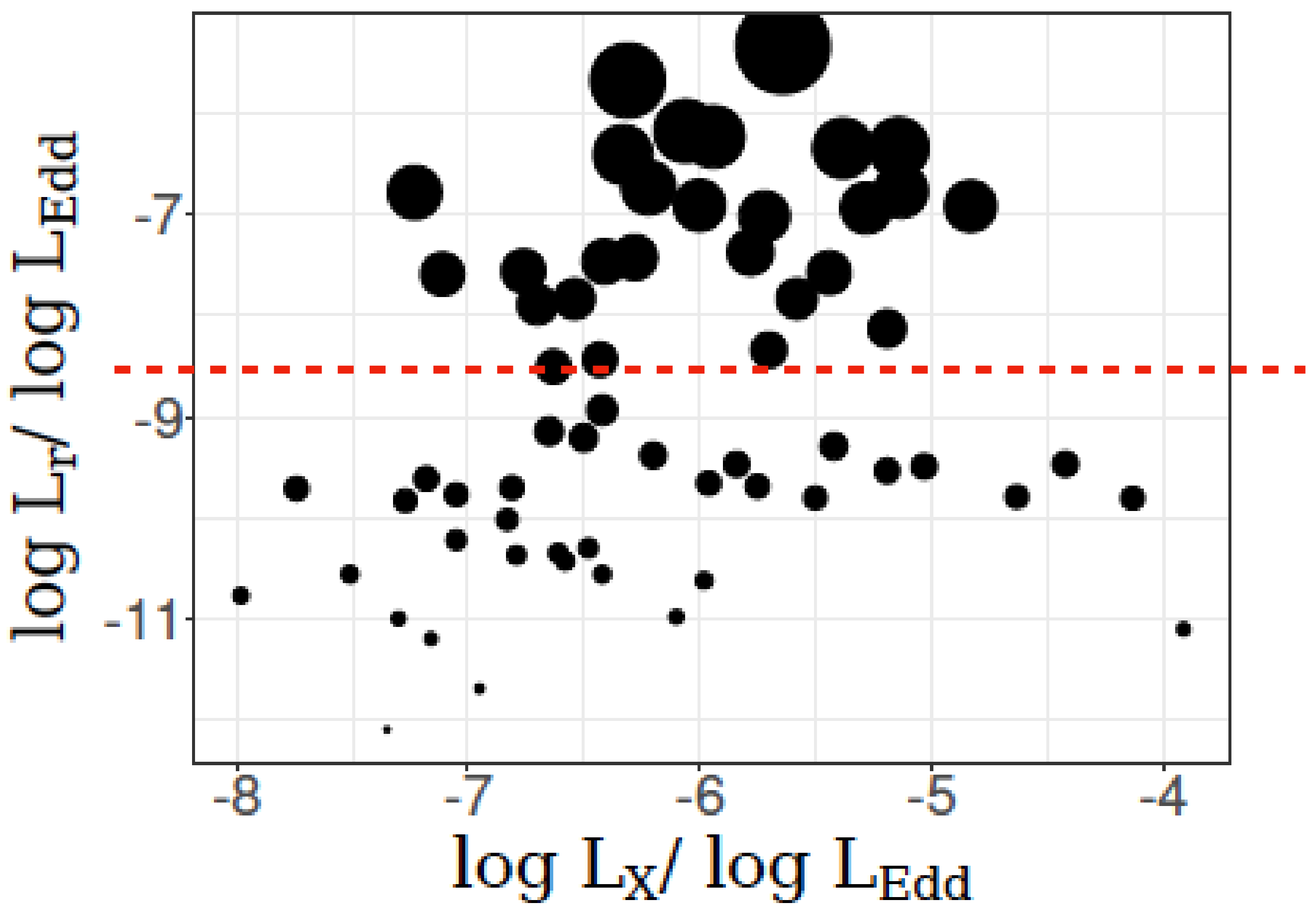

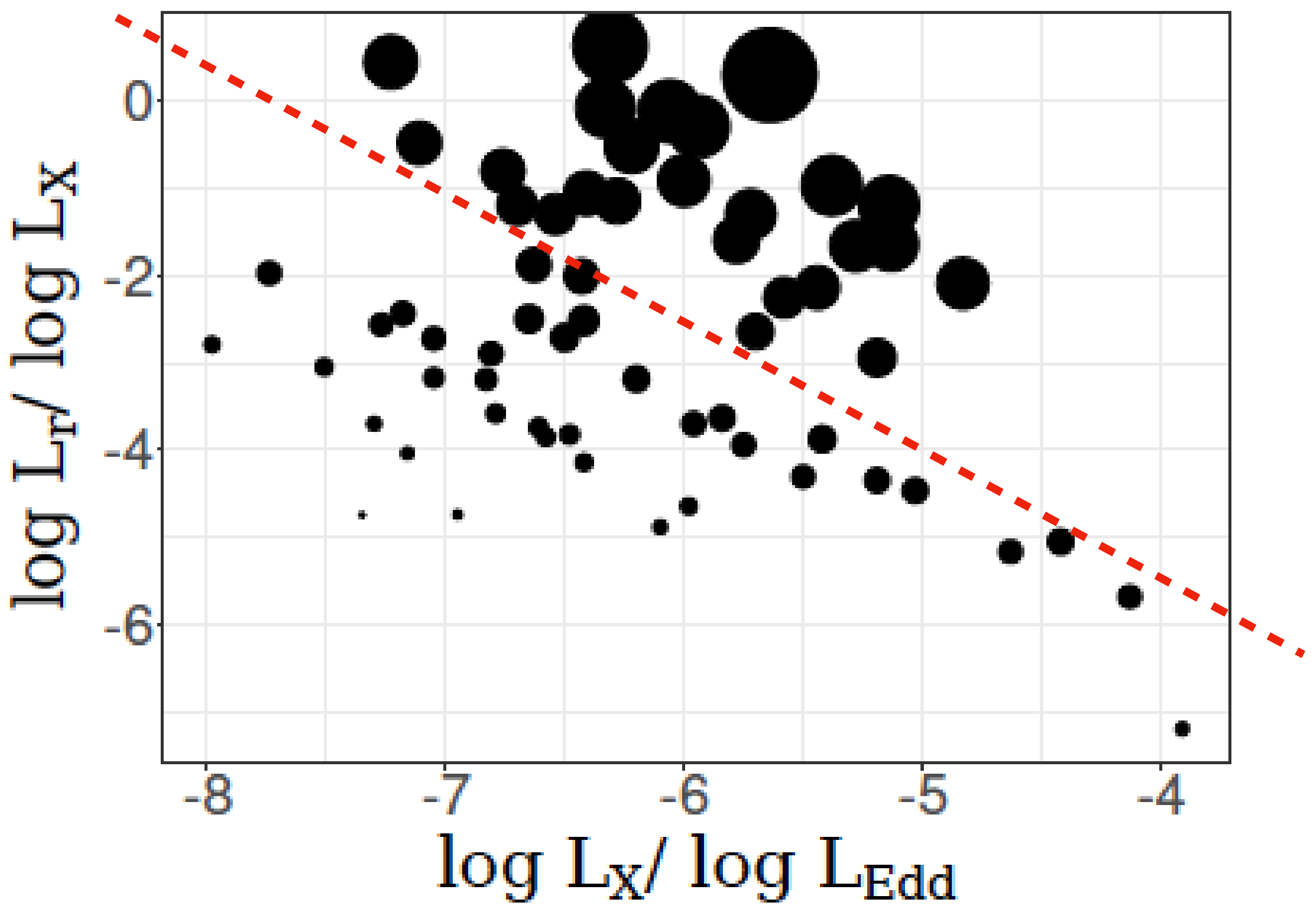

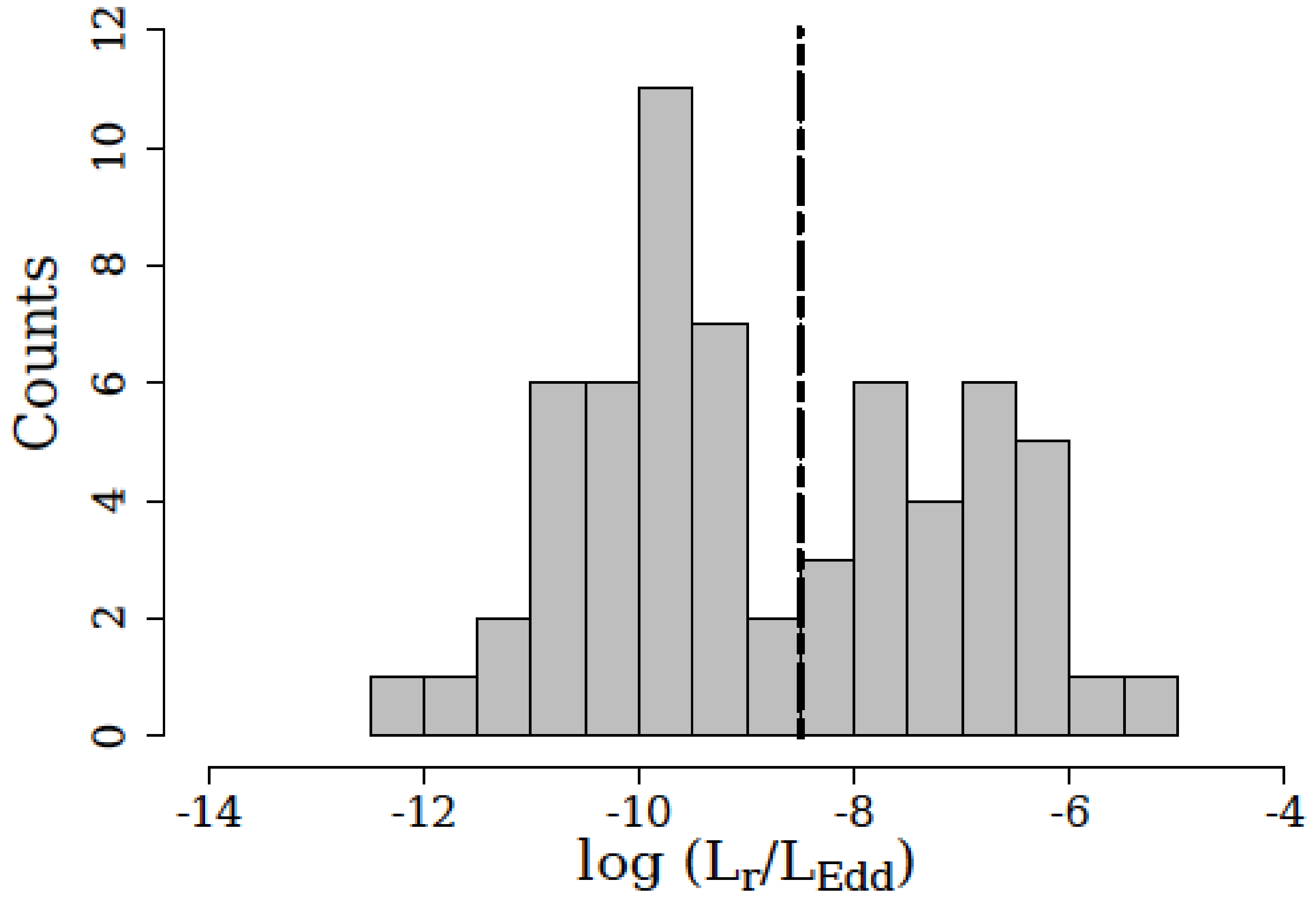

RESULTS:

However…

A closer inspection reveals a clear separation between “radio-dim” and “radio-bright” early-type galaxies

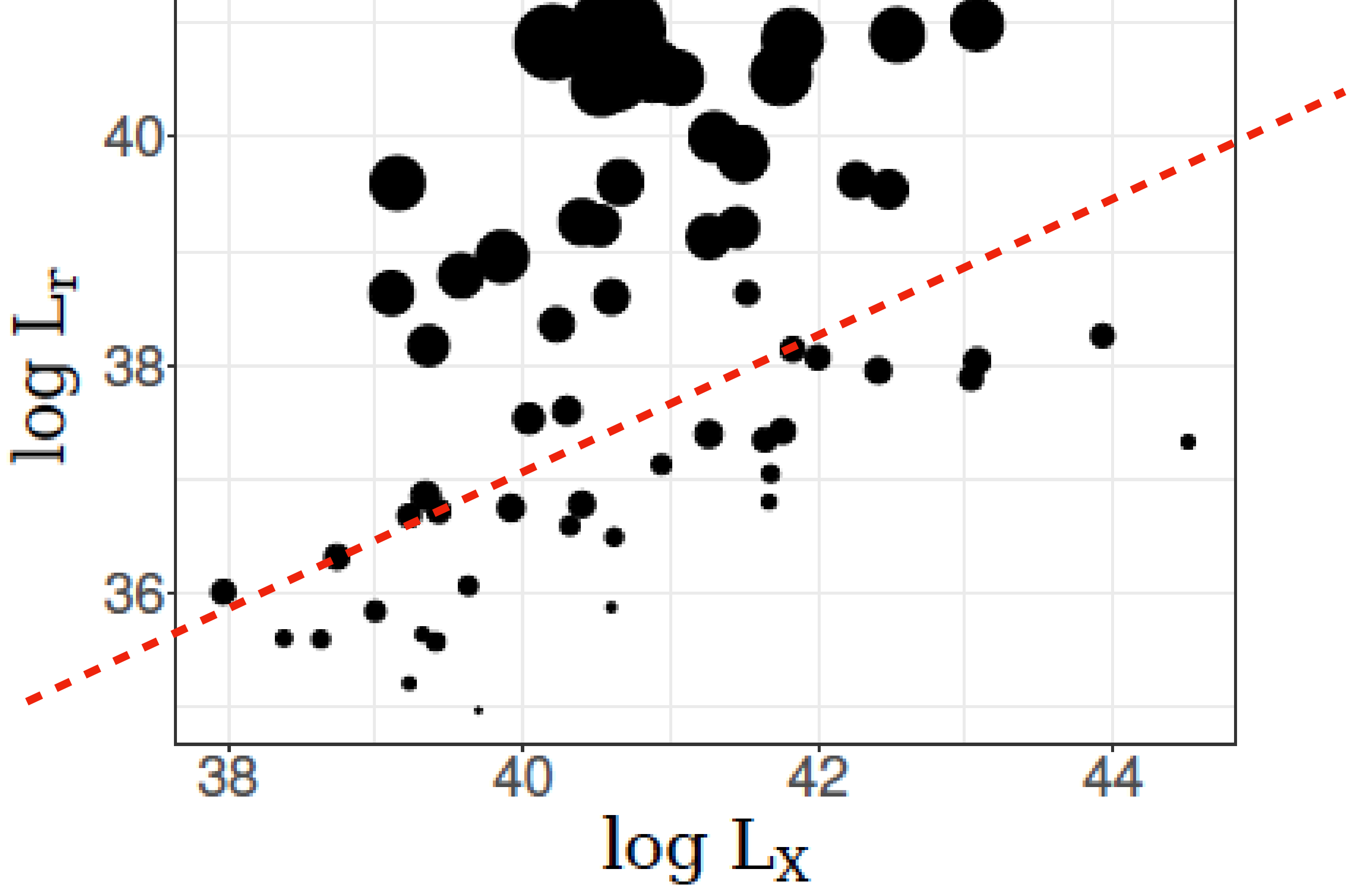

Graph for early-type sources only; the size of the points reflects L_r/L_Edd

A bi-modial distribution ?!

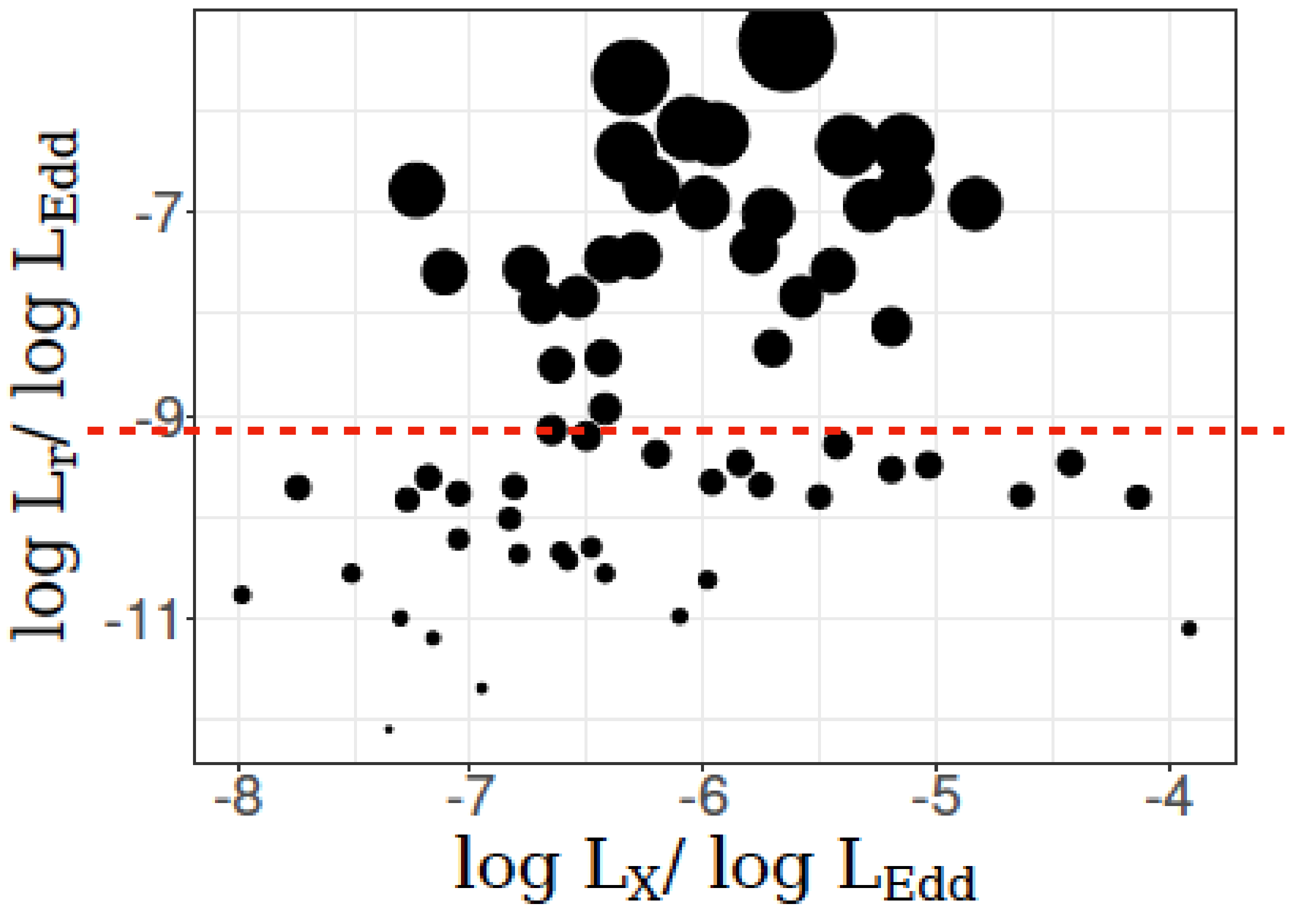

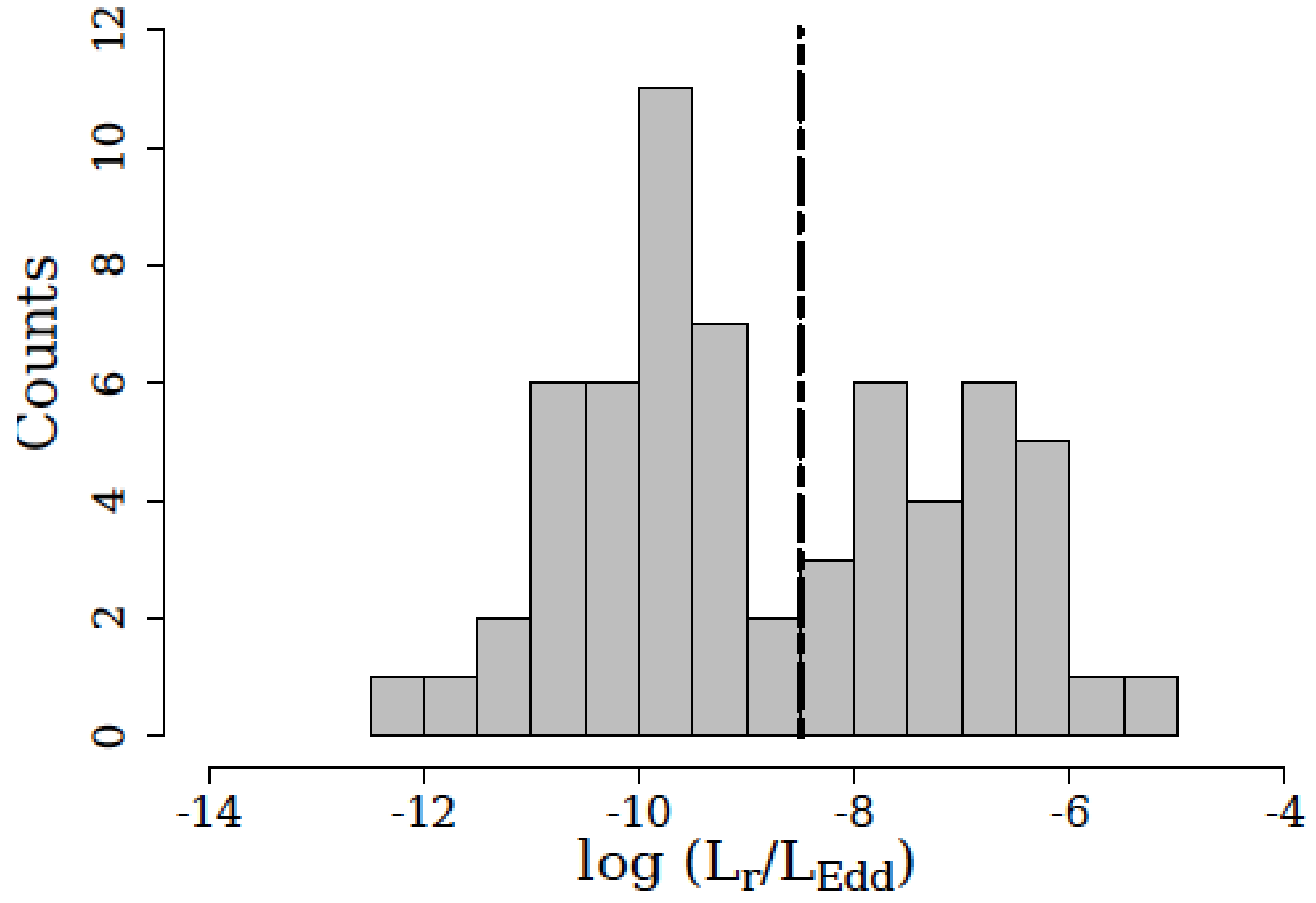

modetest function the CRAN “multimode" package within the R statistical software environment.

This function tests the number of modes in observed data set. null hypothesis were tested, assuming that the true number of modes is equal to mod0 = 1 and mod0 = 2.

According to (Ameijeiras-Alonso et al. 2016) excess mass test we cannot rule out the hypothesis that true number of modes is equal to mod0 = 1 with p=0.14; p-value further increases if the null hypothesis is that number of mode is equal to mod0 = 2.

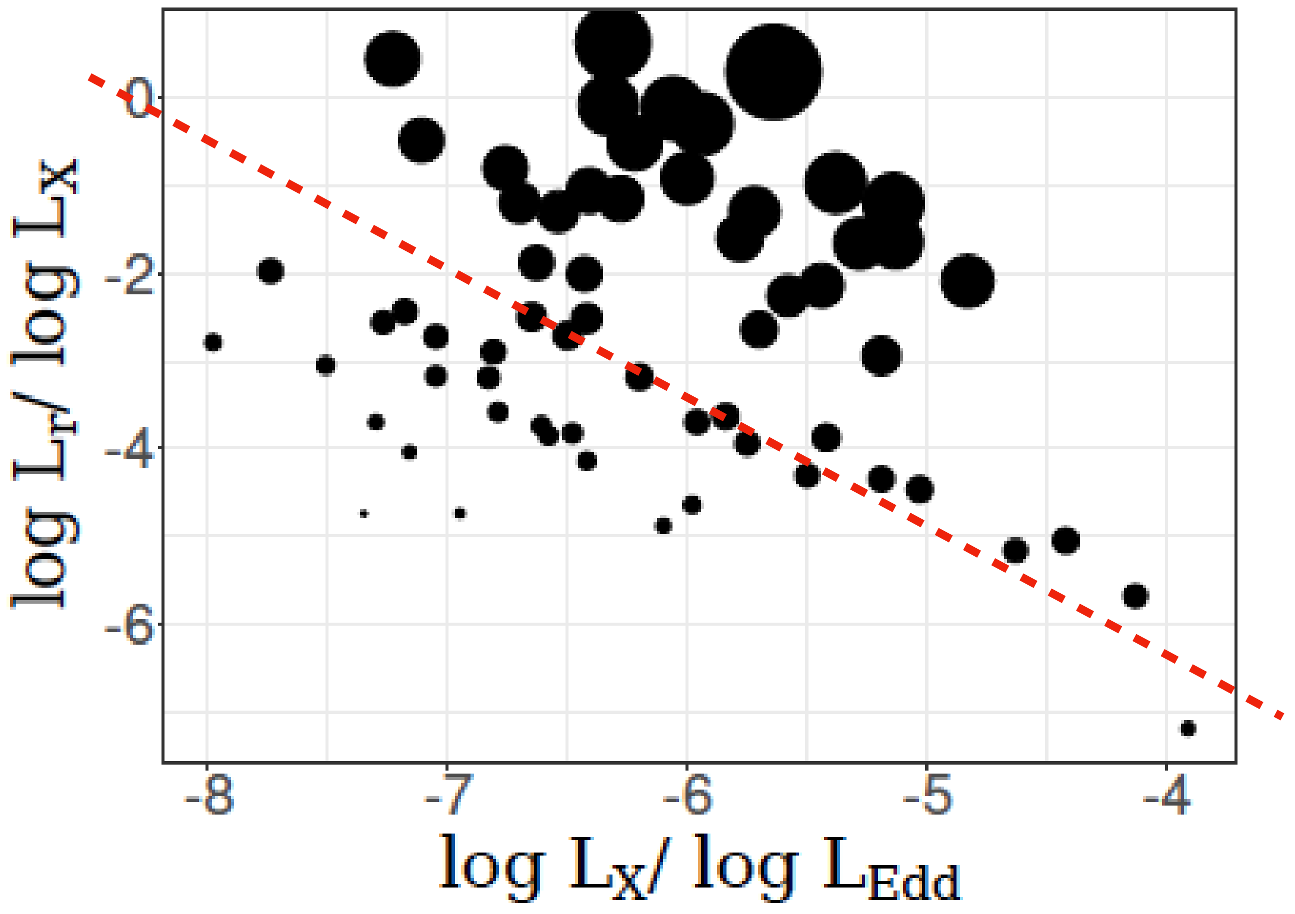

Maybe too little data… need for a large number of sources with precisely measure BH masses and week radio luminosities.

RESULTS:

Moreover…

The radio-dim and radio-bright sources correlate differently with the galactic and large-scale environment parameters

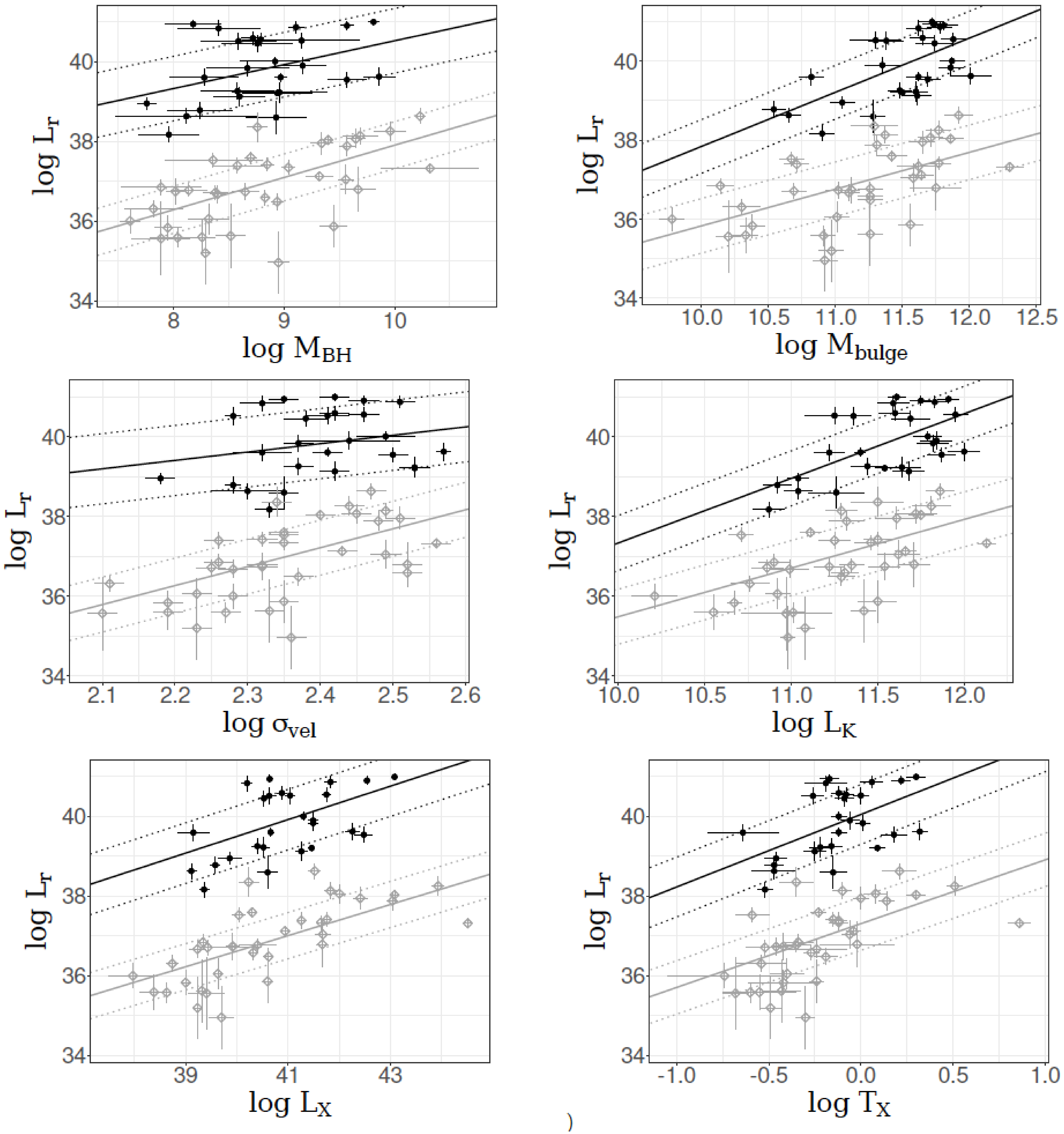

RESULTS:

Moreover…

The radio-dim and radio-bright sources correlate differently with the galactic and large-scale environment parameters

In this work we investigate the univariate linear regression using the APEMoST[2] algorithm (Gruberbauer et al. 2009) . We assume the linear trend: $Y \sim a + b \cdot X + \epsilon$, with a normally distributed noise $\epsilon \sim \mathcal{N}(0, \sigma)$, $Y-$ vector of responses an $X-$ vector of the predictor variable. The standard deviation of the noise distribution σ can be expressed as the product of combine uncertainty:

$$\sigma = \left(\sum_{i=1}^{n} (\sigma_{int}^2 + \sigma_{Y_i}^2 + (b \cdot \sigma_{X_i})^2 \right)^{\frac{1}{2}}$$

where $\sigma_{int}-$ intrinsic spread, $\sigma_{X_i}-$uncertainity associated with x_i measurments, and $\sigma_{Y_i}-$ uncertainity associated with y_i measurment.

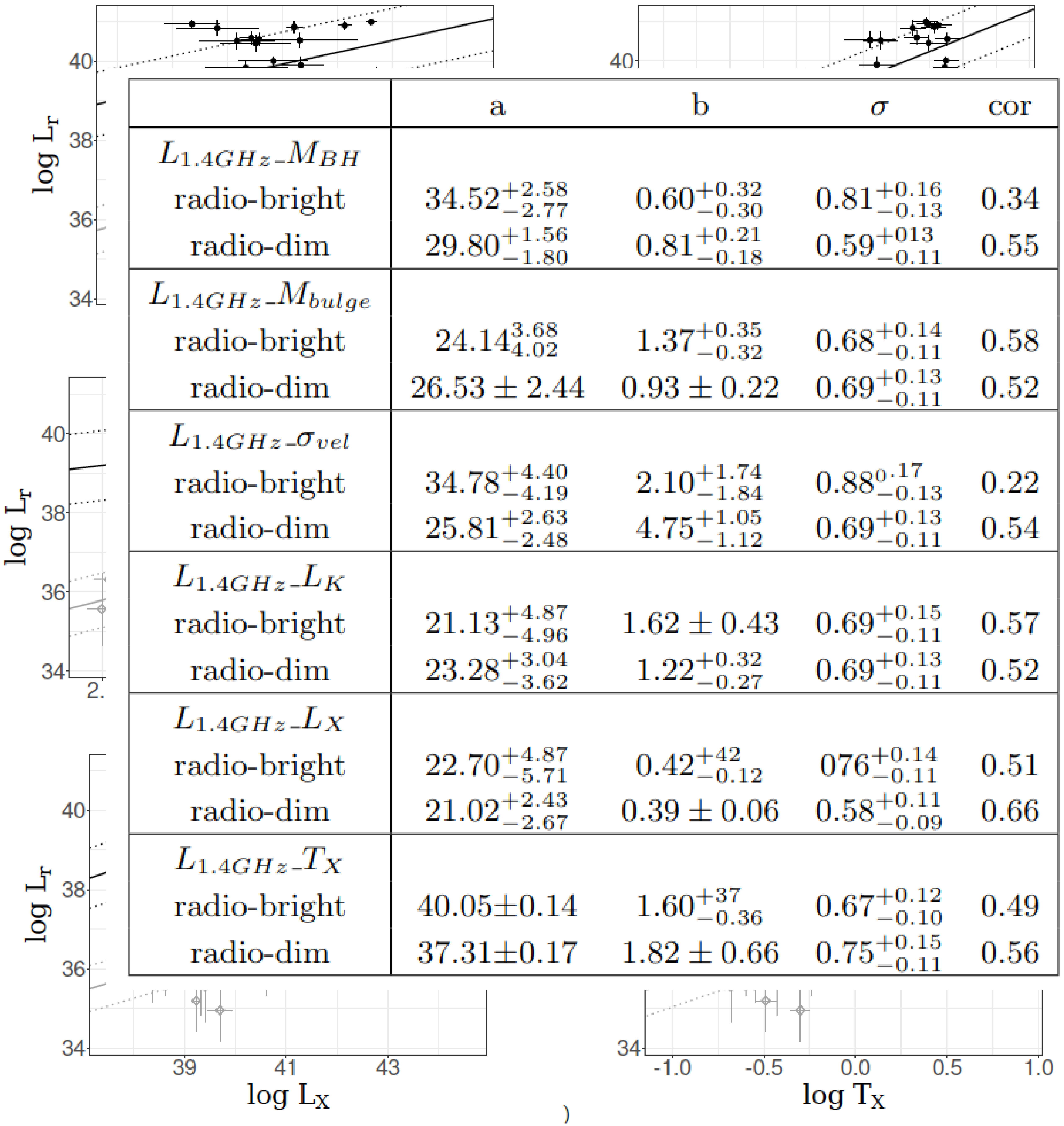

	a	b	σ	cor
$L_{1.4GHz}$-M_{BH}				
radio-bright	$34.52^{+2.58}_{-2.77}$	$0.60^{+0.32}_{-0.30}$	$0.81^{+0.16}_{-0.13}$	0.34
radio-dim	$29.80^{+1.56}_{-1.80}$	$0.81^{+0.21}_{-0.18}$	$0.59^{+013}_{-0.11}$	0.55
$L_{1.4GHz}$-M_{bulge}				
radio-bright	$24.14^{3.68}_{4.02}$	$1.37^{+0.35}_{-0.32}$	$0.68^{+0.14}_{-0.11}$	0.58
radio-dim	26.53 ± 2.44	0.93 ± 0.22	$0.69^{+0.13}_{-0.11}$	0.52
$L_{1.4GHz}$-σ_{vel}				
radio-bright	$34.78^{+4.40}_{-4.19}$	$2.10^{+1.74}_{-1.84}$	$0.88^{0.17}_{-0.13}$	0.22
radio-dim	$25.81^{+2.63}_{-2.48}$	$4.75^{+1.05}_{-1.12}$	$0.69^{+0.13}_{-0.11}$	0.54
$L_{1.4GHz}$-L_K				
radio-bright	$21.13^{+4.87}_{-4.96}$	1.62 ± 0.43	$0.69^{+0.15}_{-0.11}$	0.57
radio-dim	$23.28^{+3.04}_{-3.62}$	$1.22^{+0.32}_{-0.27}$	$0.69^{+0.13}_{-0.11}$	0.52
$L_{1.4GHz}$-L_X				
radio-bright	$22.70^{+4.87}_{-5.71}$	$0.42^{+42}_{-0.12}$	$076^{+0.14}_{-0.11}$	0.51
radio-dim	$21.02^{+2.43}_{-2.67}$	0.39 ± 0.06	$0.58^{+0.11}_{-0.09}$	0.66
$L_{1.4GHz}$-T_X				
radio-bright	40.05 ± 0.14	$1.60^{+37}_{-0.36}$	$0.67^{+0.12}_{-0.10}$	0.49
radio-dim	37.31 ± 0.17	1.82 ± 0.66	$0.75^{+0.15}_{-0.11}$	0.56

RESULTS:

Moreover…

The radio-dim and radio-bright sources correlate differently with the galactic and large-scale environment parameters

In this work we investigate the univariate linear regression using the APEMoST[2] algorithm (Gruberbauer et al. 2009) . We assume the linear trend: $Y \sim a + b \cdot X + \epsilon$, with a normally distributed noise $\epsilon \sim \mathcal{N}(0, \sigma)$, $Y-$ vector of responses an $X-$ vector of the predictor variable. The standard deviation of the noise distribution σ can be expressed as the product of combine uncertainty:

$$\sigma = \left(\sum_{i=1}^{n} (\sigma_{int}^2 + \sigma_{Y_i}^2 + (b \cdot \sigma_{X_i})^2 \right)^{\frac{1}{2}}$$

where $\sigma_{int}-$ intrinsic spread, $\sigma_{X_i}-$uncertainity associated with x_i measurments, and $\sigma_{Y_i}-$ uncertainity associated with y_i measurment.

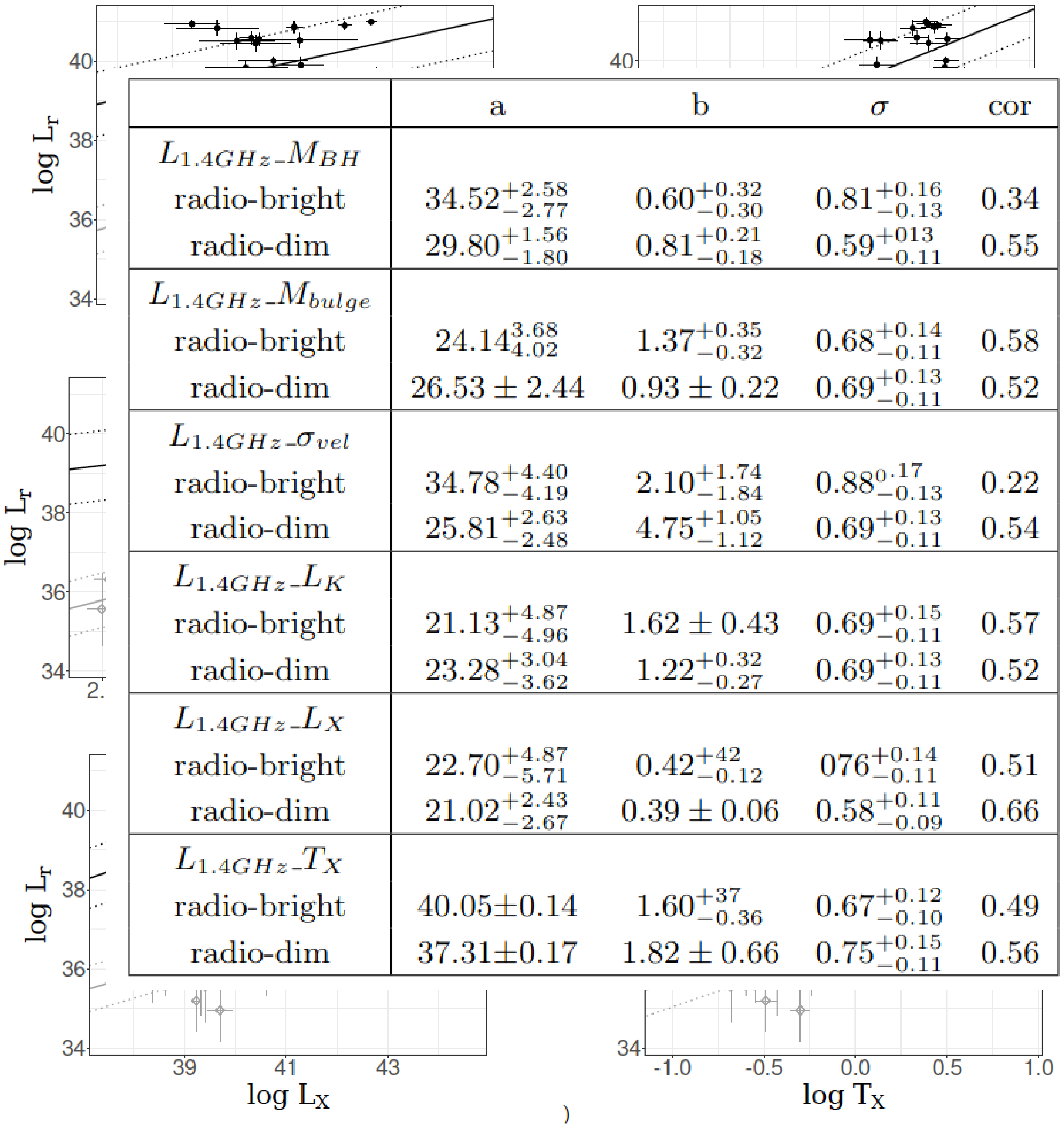

	a	b	σ	cor
$L_{1.4GHz}$-M_{BH}				
radio-bright	$34.52^{+2.58}_{-2.77}$	$0.60^{+0.32}_{-0.30}$	$0.81^{+0.16}_{-0.13}$	0.34
radio-dim	$29.80^{+1.56}_{-1.80}$	$0.81^{+0.21}_{-0.18}$	$0.59^{+013}_{-0.11}$	0.55
$L_{1.4GHz}$-M_{bulge}				
radio-bright	$24.14^{3.68}_{4.02}$	$1.37^{+0.35}_{-0.32}$	$0.68^{+0.14}_{-0.11}$	0.58
radio-dim	26.53 ± 2.44	0.93 ± 0.22	$0.69^{+0.13}_{-0.11}$	0.52
$L_{1.4GHz}$-σ_{vel}				
radio-bright	$34.78^{+4.40}_{-4.19}$	$2.10^{+1.74}_{-1.84}$	$0.88^{0.17}_{-0.13}$	0.22
radio-dim	$25.81^{+2.63}_{-2.48}$	$4.75^{+1.05}_{-1.12}$	$0.69^{+0.13}_{-0.11}$	0.54
$L_{1.4GHz}$-L_K				
radio-bright	$21.13^{+4.87}_{-4.96}$	1.62 ± 0.43	$0.69^{+0.15}_{-0.11}$	0.57
radio-dim	$23.28^{+3.04}_{-3.62}$	$1.22^{+0.32}_{-0.27}$	$0.69^{+0.13}_{-0.11}$	0.52
$L_{1.4GHz}$-L_X				
radio-bright	$22.70^{+4.87}_{-5.71}$	$0.42^{+42}_{-0.12}$	$076^{+0.14}_{-0.11}$	0.51
radio-dim	$21.02^{+2.43}_{-2.67}$	0.39 ± 0.06	$0.58^{+0.11}_{-0.09}$	0.66
$L_{1.4GHz}$-T_X				
radio-bright	40.05 ± 0.14	$1.60^{+37}_{-0.36}$	$0.67^{+0.12}_{-0.10}$	0.49
radio-dim	37.31 ± 0.17	1.82 ± 0.66	$0.75^{+0.15}_{-0.11}$	0.56

RESULTS:

A work in progress:

Nuclear X-ray luminosities (extracted from the innermost 2.5’’ regions with Chandra; see She et al. 2017)
→
expected to correspond to the emission of accretion disks and disk coronae, and as such to give us some clues on the current accretion rates.

No very obvious difference between radio-dim and radio-bright sources (possibly only a higher median for radio-bright) although this analysis is still very preliminary

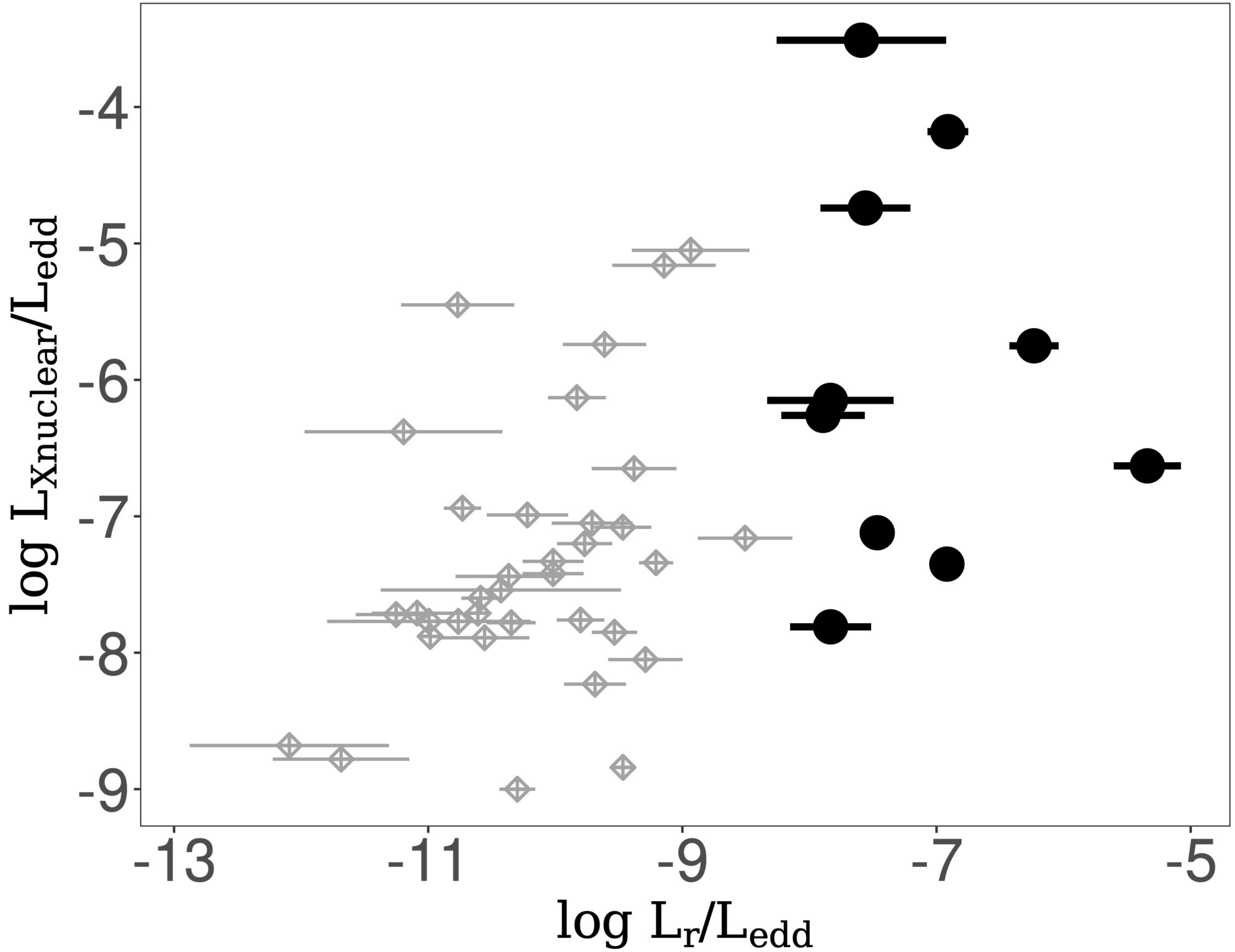

RESULTS:

Finally…

A tight FIR-radio correlation is established in all the starforming systems; in the case of the objects analyzed here, one could expect this correlation to hold at least for radio-dim sources, for which the observed radio emission should most likely correspond to a residual starformation within the central regions of galaxies.

But no tight correlations are observed for either radio-dim or radio-bright sources…

	cor	p-value
Lr vs L60_bright	**-0.05**	**0.83**
Lr vs L60_dim	**0.22**	**0.31**
Lr vs L60_bright	**-0.20**	**0.44**
Lr vs L60_dim	**0.24**	**0.26**
Lr vs FIR_bright	**-0.24**	**0.34**
Lr vs FIR_dim -	**0.31**	**0.14**

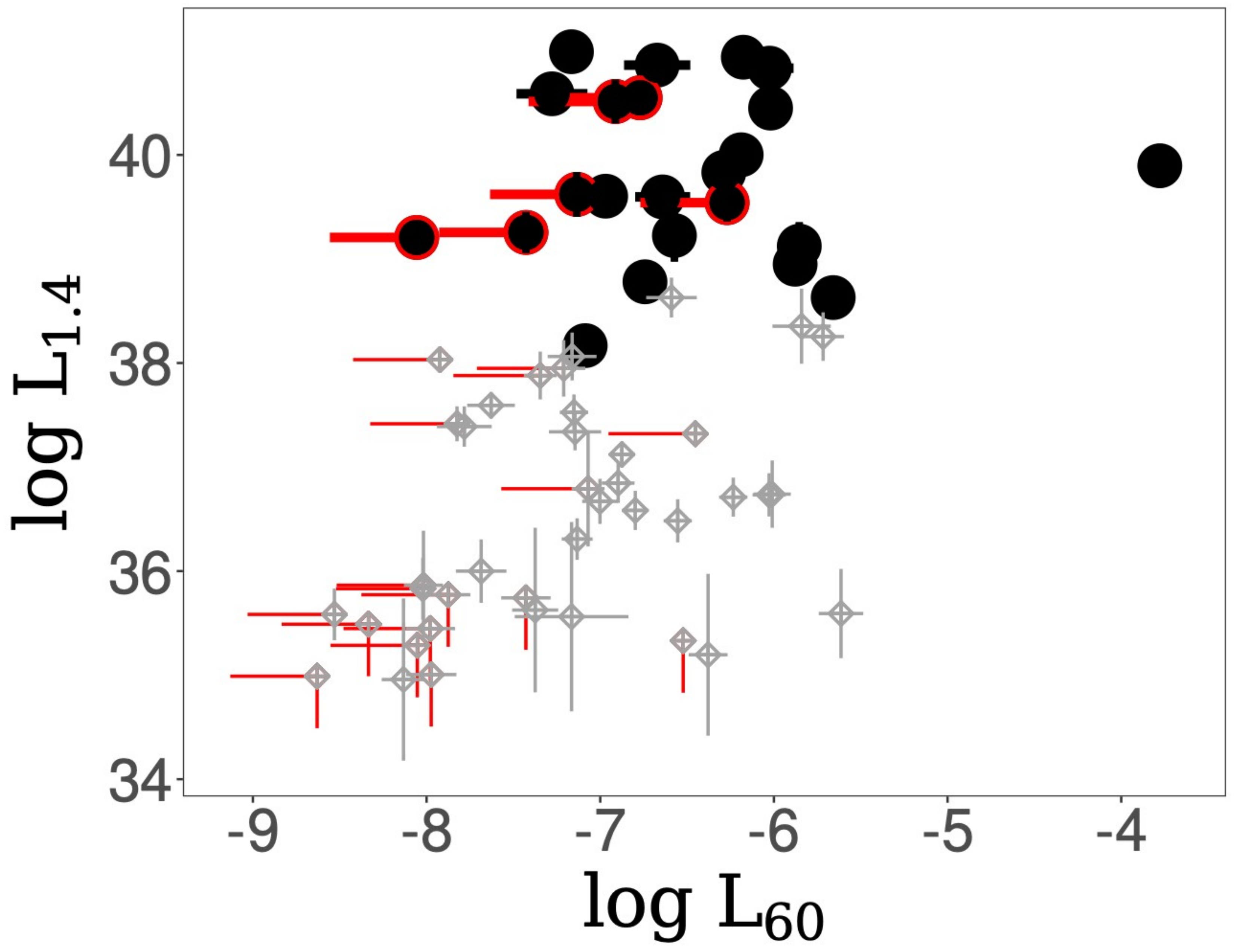

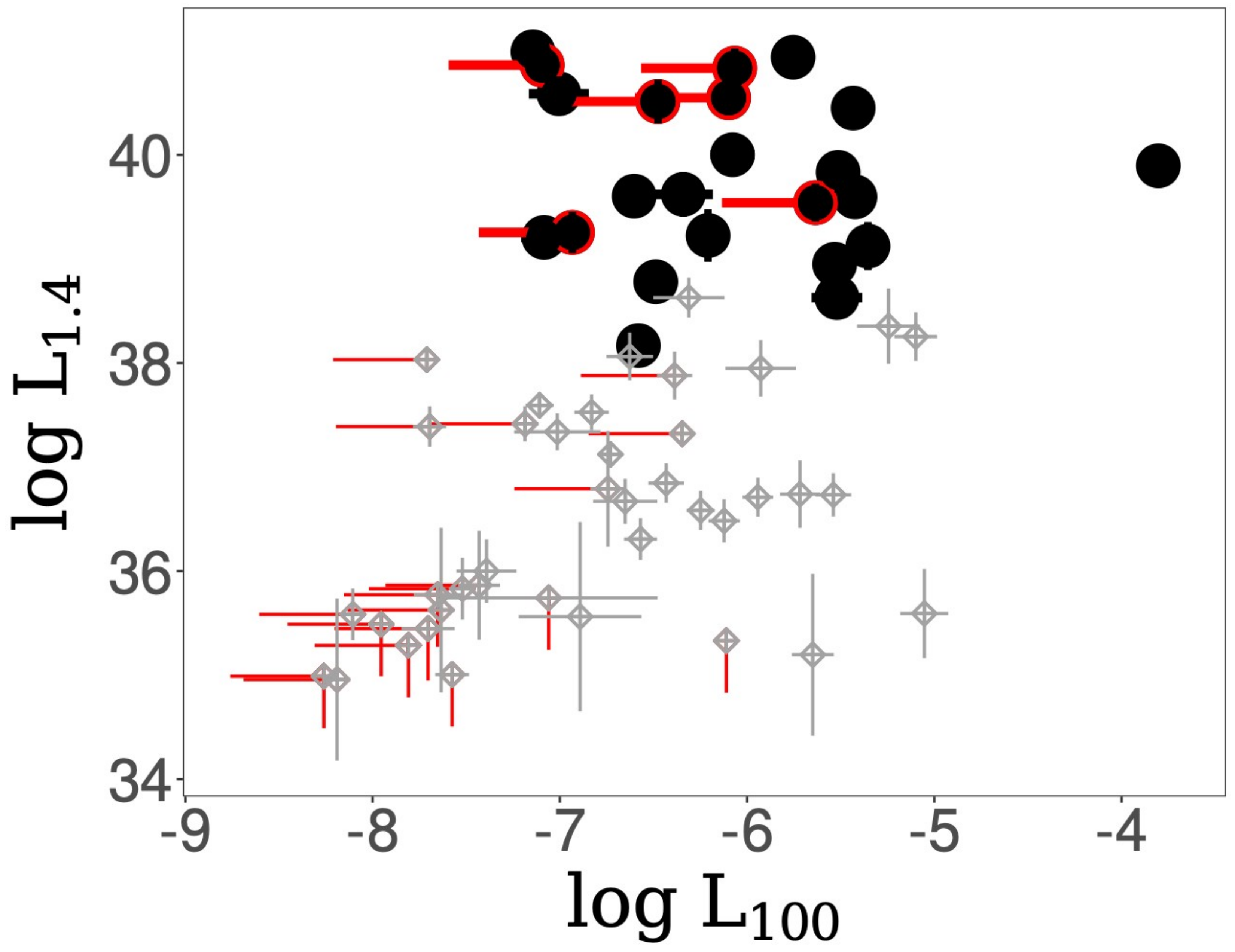

RESULTS:

Finally…

A tight FIR-radio correlation is established in all the starforming systems; in the case of the objects analyzed here, one could expect this correlation to hold at least for radio-dim sources, for which the observed radio emission should most likely correspond to a residual starformation within the central regions of galaxies.

But no tight correlations are observed for either radio-dim or radio-bright sources…

… situation improves if we include only sources listed in IRAS Galaxy Catalog

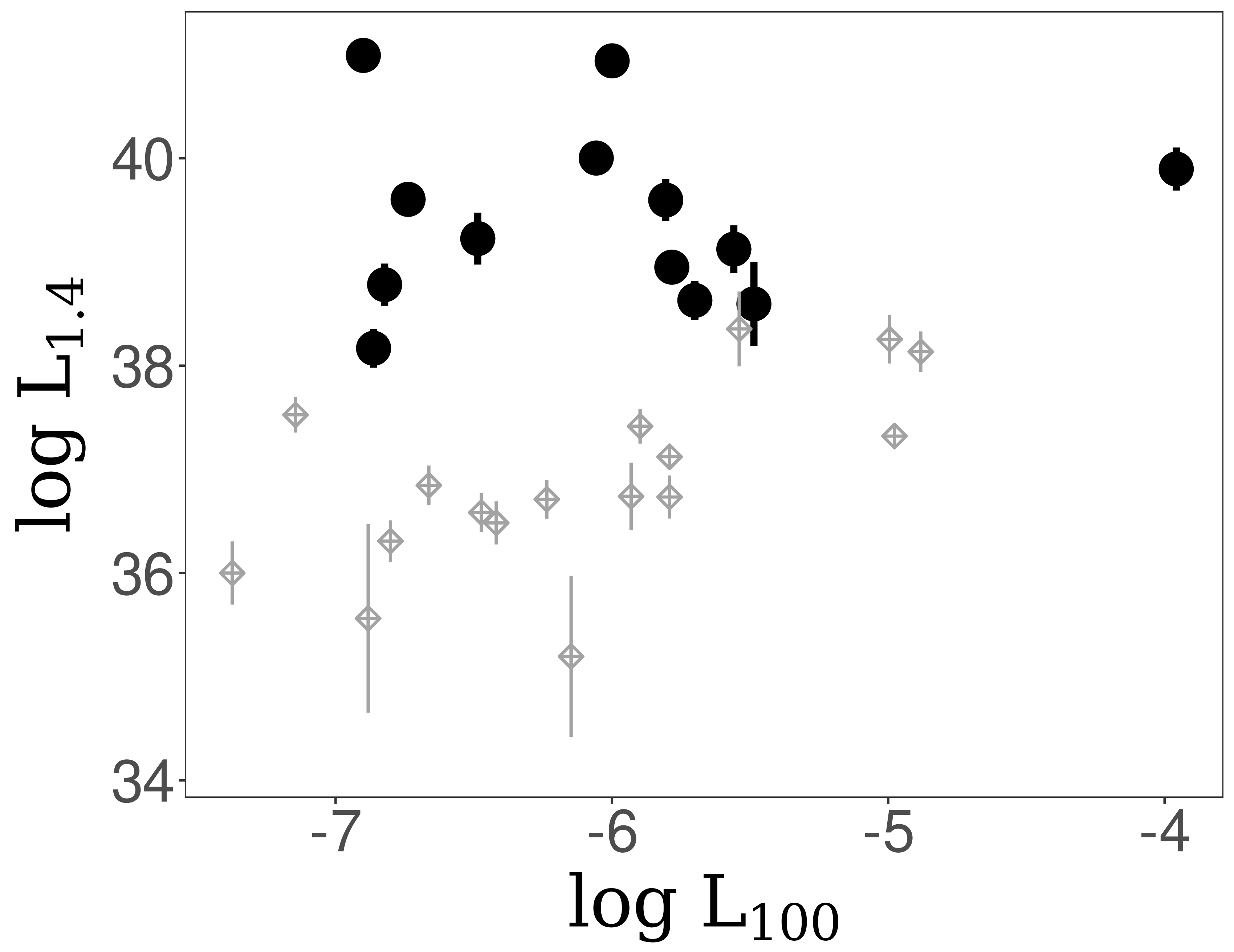

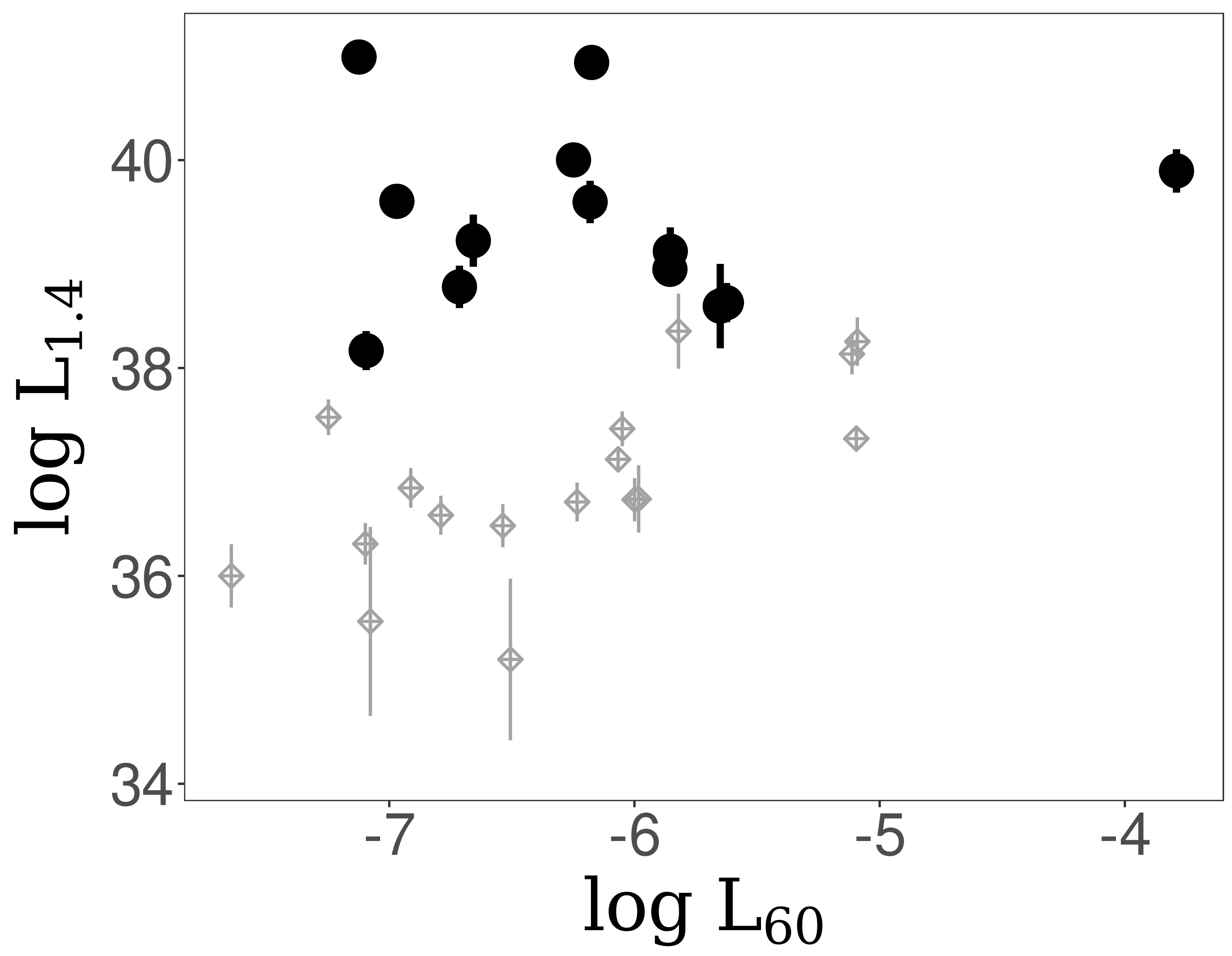

RESULTS:

$$q \equiv \log\left(\frac{\mathrm{FIR}}{3.75\times10^{12}\ \mathrm{W\ m^{-2}}}\right) - \log\left(\frac{S_{1.4\ \mathrm{GHz}}}{\mathrm{W\ m^{-2}\ Hz^{-1}}}\right)$$

Instead…

We see that the q parameter correlates with SMBH mass for radio-dim sources, and galactic bulge mass for radio-bright sources…

Although the above-mentioned correlations are rather marginal…

	cor	**p-value**
MBH vs q bright	**-0.46**	**0.06**
MBH vs q dim	**-0.46**	**0.02**
Mbulge vs q bright	**-0.58**	**0.01**
Mbulge vs q dim	**-0.34**	**0.11**

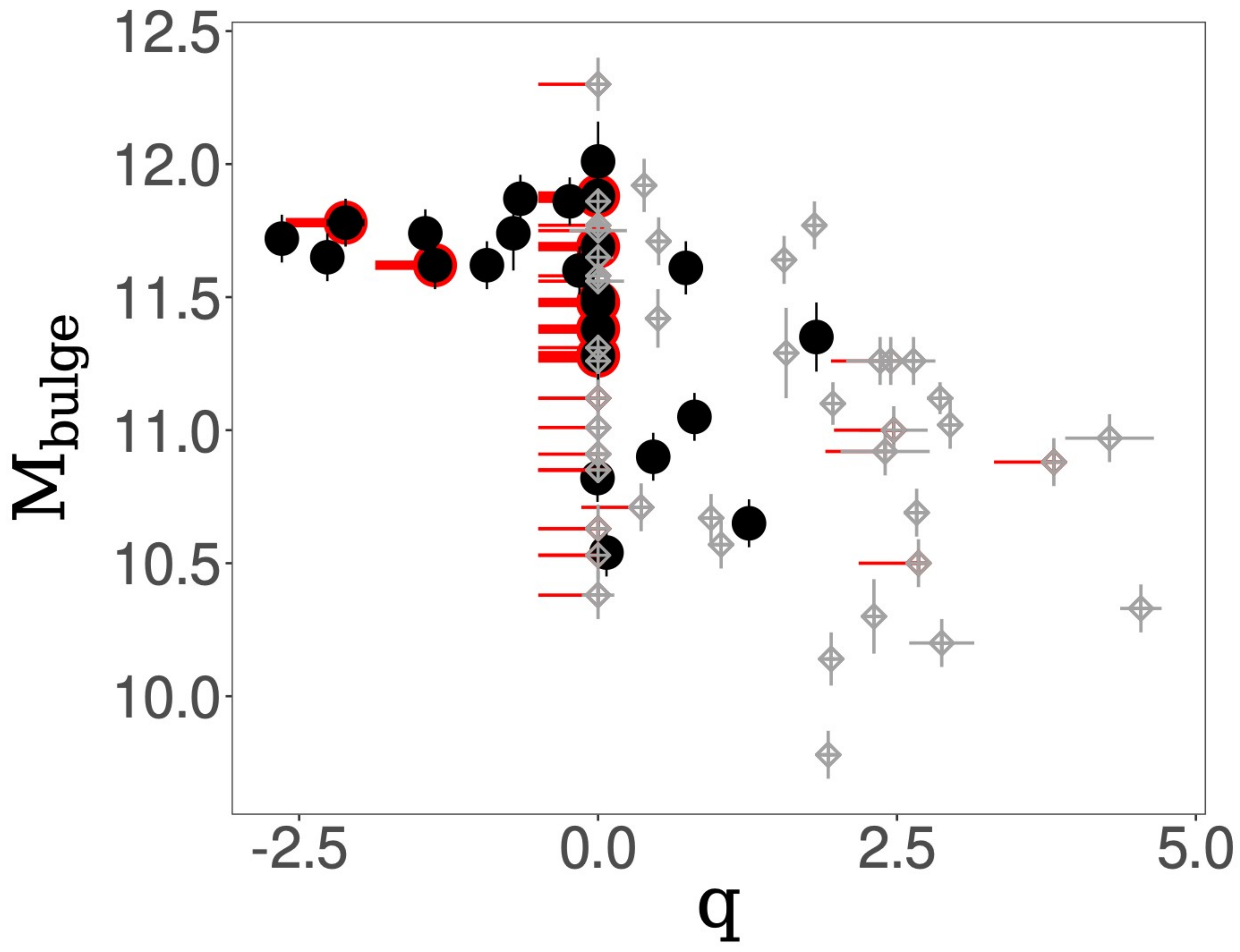

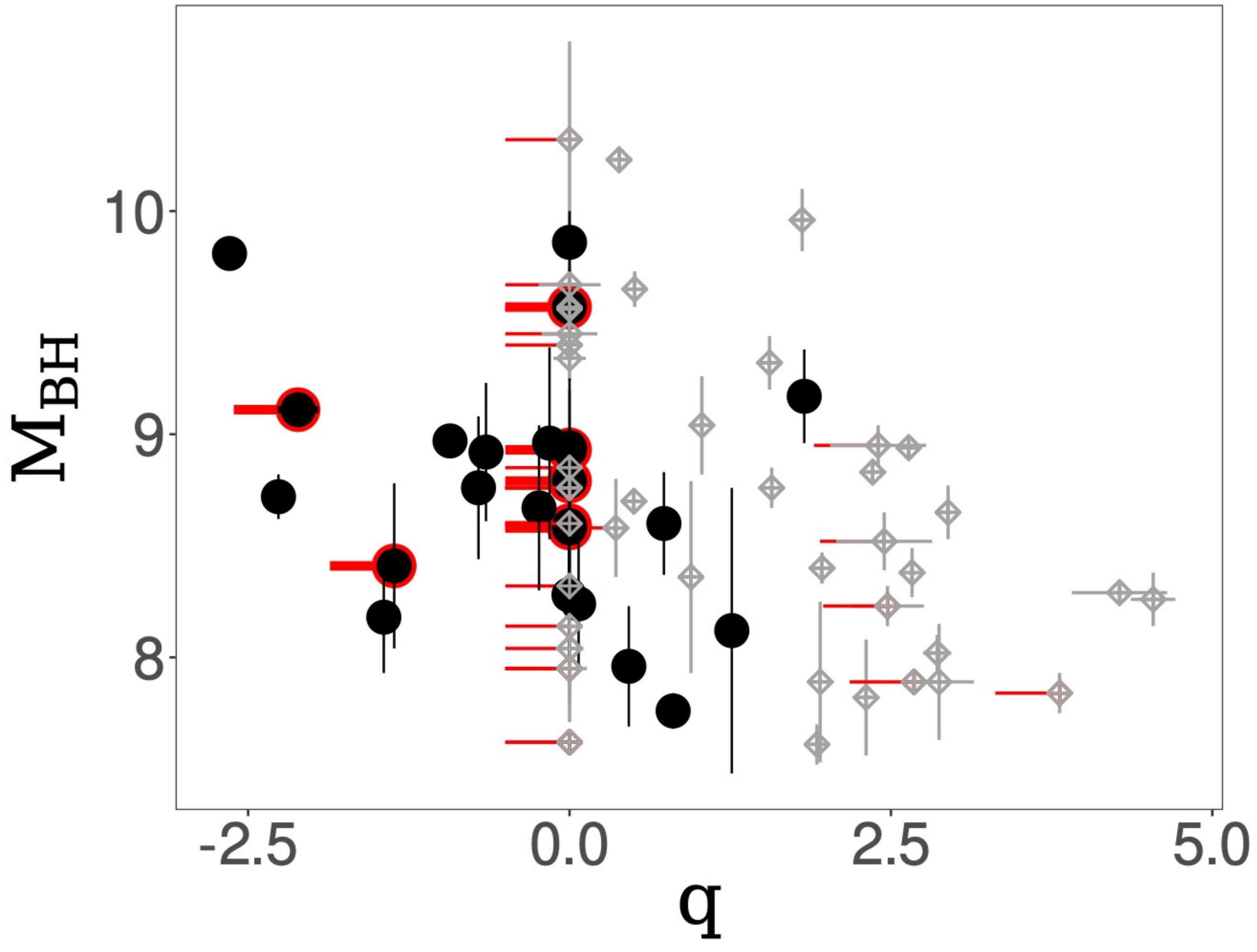

RESULTS:

$$q \equiv \log\left(\frac{\mathrm{FIR}}{3.75 \times 10^{12}\ \mathrm{W\ m^{-2}}}\right) - \log\left(\frac{S_{1.4\ \mathrm{GHz}}}{\mathrm{W\ m^{-2}\ Hz^{-1}}}\right)$$

Instead…

… and with the hot halo luminosity ?

	cor	p-value
Lx500/Ledd vs q bright	-0.41	0.10
Lx500/Ledd vs q dim	-0.35	0.10
Lx500 vs q bright	-0.48	0.05
Lx500 vs q dim	-0.46	0.02

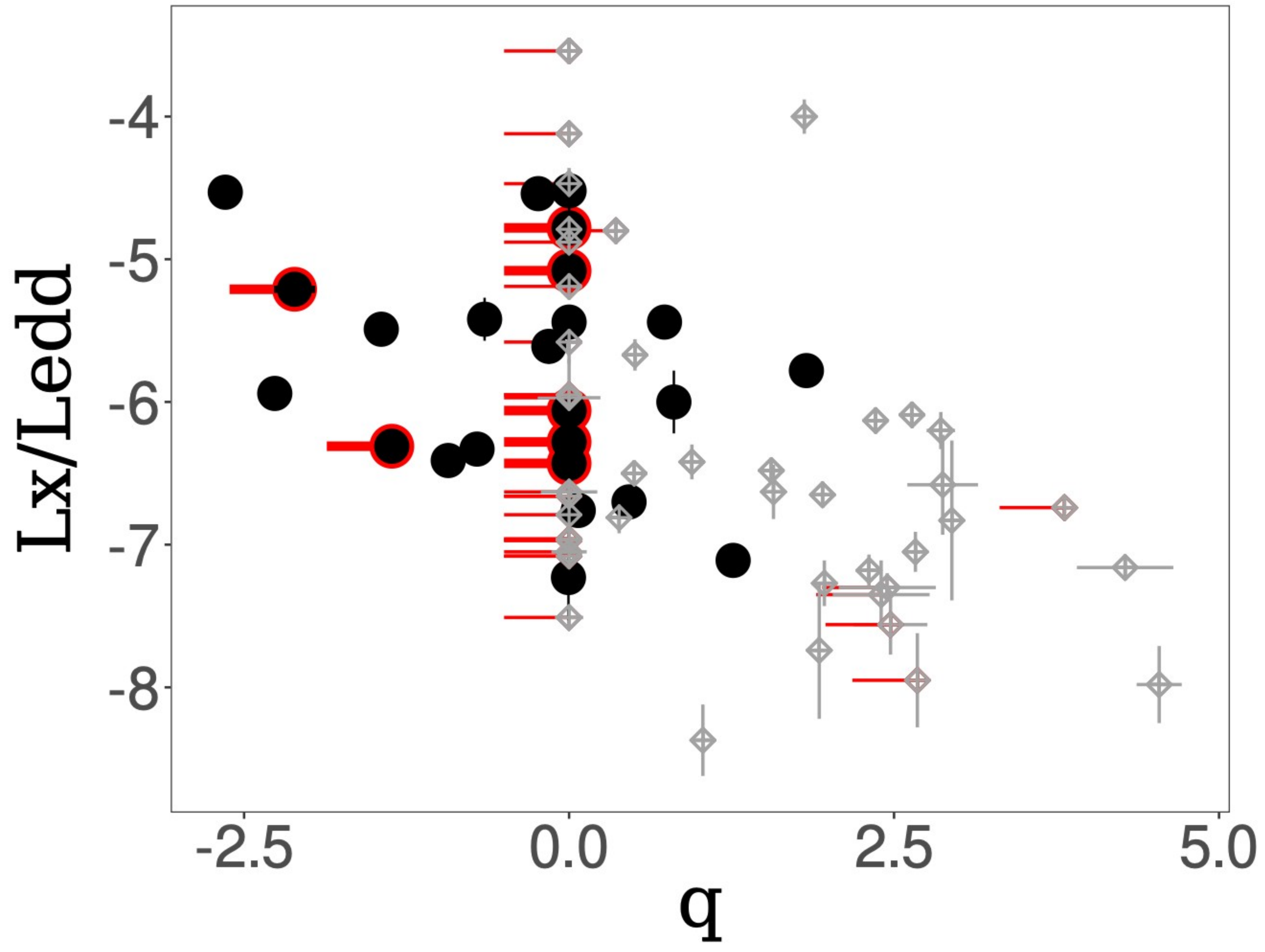

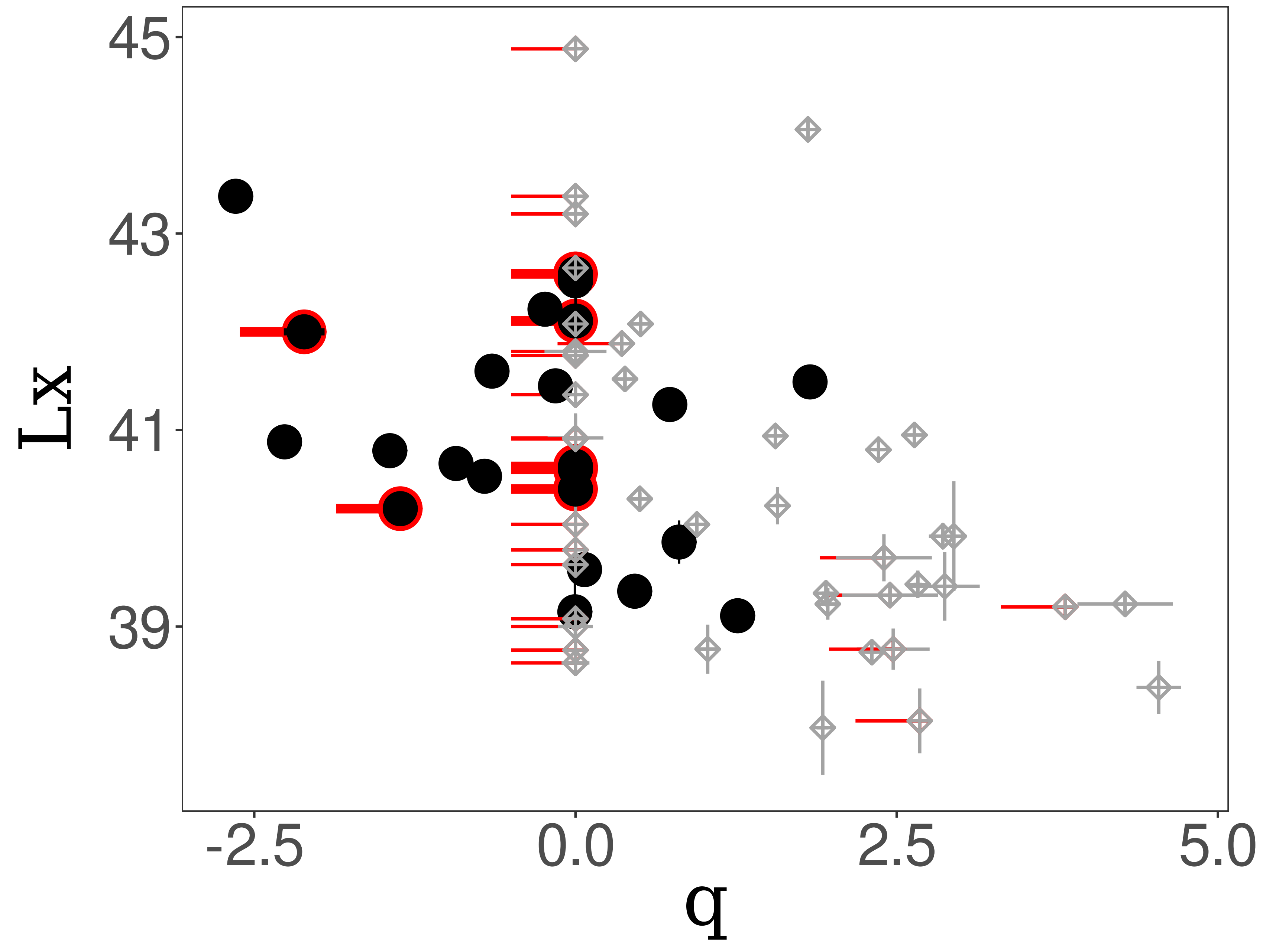

CONCLUSIONS:

a unique collection of high-quality optical and X-ray data for nearby 76 early-type galaxies:

1. possible two populations of "radio-dim" and "radio-bright" sources, with the borderline luminosity ***log L_1.4 / L_Edd ~ —8.5* ;**
2. radio-dim and radio-bright sources correlate differently with the galactic and large-scale environment parameters (stellar velocity dispersion, bulge mass, galactic luminosity, halo X-ray luminosity and temperature);
3. no indication for significant differences in current accretion rates between radio-dim or radio-bright sources from high-resolution X-ray spectroscopy;
4. no statistically significant FIR-radio correlations for either radio-dim or radio-bright sources; all radio-bright sources, but also many of radio-dim ones, are "radio excess" in a sense ***q >> 2.5* ;**
5. hints for interesting differences in correlations of the FIR-radio luminosity ratio *q* with SMBH and galactic bulge masses, as well hot halo X-ray luminosity, between radio-dim or radio-bright sources.

The work is sill in progress, and this also regard the interpretation of the obtained results… So please stay tuned !

45 Ellipticals with 1.4GHz detections
7 Ellipticals with radio ULs
3 Ellipticals with no radio information at 1.4GHz

55 Ellipticals

17 Lenticulars with 1.4GHz detections
2 Lenticulars with radio ULs
2 Lenticulars with no radio information at 1.4GHz

21 Lenticulars